Agricultural and Forest Meteorology 375 (2025) 110851

Contents lists available at ScienceDirect

Agricultural and Forest Meteorology

journal homepage: www.elsevier.com/locate/agrformet

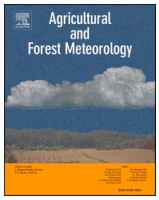

Increase in carbon sink in a protected tropical seasonal rainforest in southwestern China over 20 years

Yaqi Liu [a,b,c,1], Linjie Jiao [a,1], Jing Zhang [a,b], Xuefei Li [c], Huixu Zheng [a], Boonsiri Sawasdchai [a,b], Yaoliang Chen [d], Yiping Zhang [a], Palingamoorthy Gnanamoorthy [a,*], Qinghai Song [a,*]

[a] Yunnan Key Laboratory of Forest Ecosystem Stability and Global Change, Xishuangbanna Tropical Botanical Garden, Chinese Academy of Sciences, Mengla, Yunnan, 666303, China
[b] University of Chinese Academy of Sciences, Beijing 100049, China
[c] Institute for Atmospheric and Earth System Research/Physics, Faculty of Science, University of Helsinki, Helsinki 00014, Finland
[d] School of Geographical Sciences, Fujian Normal University, Fuzhou 350007, China

ARTICLE INFO

Keywords:
Tropical rainforest
Eddy covariance
CO_2 flux
Carbon sink
Southwestern Asia

ABSTRACT

Tropical forests play a significant role in the global carbon cycle, but the lack of long-term in-situ datasets renders our understanding of the specific carbon dynamics in tropical forests uncertain. This study investigated the long-term trends (from 2003 to 2022) in gross primary productivity (GPP), ecosystem respiration (Reco), and net ecosystem productivity (NEP) at a primary tropical rainforest reserve in Xishuangbanna, southwest China based on the eddy covariance technique. Our study found this protected tropical seasonal rainforest to be a modest carbon sink (annual mean NEP = 157.9 ± 56.7 g C m^{-2} $year^{-1}$), with a NEP growth rate of 3.4 % $year^{-1}$ and a similar upward trend of annual mean carbon use efficiency (CUE) (annual mean CUE = 5.9 % ± 1.8 %, growth rate = 2.4 % $year^{-1}$). The increase in NEP was mainly due to the rising trend in GPP, which averaged 2658.1 ± 254.5 g C m^{-2} $year^{-1}$ and grew at 1.0 % $year^{-1}$. With the same 6-month duration, the tropical seasonal rainforest exhibited a stronger carbon sink during the dry season (148.3 g C m^{-2} $season^{-1}$) than during the rainy season, with the dry season accounting for 93.9 % of the annual carbon sink. The enhanced dry season radiation and precipitation throughout the two decades positively affected the upward trend of the carbon sink. These findings underscore the potential of well-protected primary tropical rainforests to act as carbon sinks in the long run, contributing to future carbon budget predictions for the tropical region.

1. Introduction

Terrestrial carbon sinks have increased in the past few decades, partially mitigating climate change (Fernández-Martínez et al., 2019; Pan et al., 2024; Ruehr et al., 2023; Ueyama et al., 2024). However, under the threat of future climate change, uncertainties in the assessment of terrestrial carbon sinks may increase, posing challenges to achieving nature-based solutions for climate change mitigation (NCS) (IPBES-IPCC, 2020; IPCC, 2023; Marvin et al., 2023; Mori et al., 2021). The tropical forest ecosystem as an integral part of the terrestrial ecosystem captures around 72 Pg C from the atmosphere through photosynthesis every year and stores approximately 471 ± 93 Pg C, accounting for 55 % of global forest carbon stocks (Beer et al., 2010; Malhi, 2012; Pan et al., 2011). Tropical forests have a potential biophysical feedback to the climate, and their carbon cycle is sensitive to climate change (Carvalhais et al., 2014; Lyu et al., 2021; Rodda et al., 2021; Lawrence et al., 2022). Tropical forest carbon sinks are shaped by multiple factors, including climate change (Hubau et al., 2020; Mitchard, 2018), deforestation (Feng et al., 2022), and elevated carbon dioxide (CO_2) concentration (Ruehr et al., 2023). However, their long-term trends exhibit continental variation due to differential responses to these drivers (Hubau et al., 2020; Lewis et al., 2009; Sanwangsri et al., 2018). To date, a definitive conclusion of CO_2 exchange dynamics in various tropical forest ecosystems remains elusive.

Among all types of tropical forests, primary or old-growth tropical forests have unique value, as they store around 35 % more carbon than other tropical forests do, and they have various irreplaceable ecosystem functions (Mackey et al., 2020). Over the past few decades, the tropical

* Corresponding authors.
E-mail addresses: gnanamoorthy@xtbg.ac.cn (P. Gnanamoorthy), sqh@xtbg.ac.cn (Q. Song).
[1] These authors should be considered the joint first author.

https://doi.org/10.1016/j.agrformet.2025.110851
Received 24 March 2025; Received in revised form 25 August 2025; Accepted 8 September 2025
Available online 21 September 2025

regions in Southeast Asia (SEA) have been heavily impacted by human activities, with large-scale deforestation for oil palm, rubber, and other crop plantations, leading to significant carbon loss and negative ecological effects (Clough et al., 2016; Feng et al., 2022). Therefore, long-term in-situ observation of CO_2 exchange dynamics in these primary forests of SEA provides valuable information on the long-term carbon balance within tropical forests, thereby informing research on the carbon cycle of terrestrial ecosystems and forest management policies. Meteorological factors (e.g., temperature, air, and soil moisture) reportedly have significant influences on tropical rainforest ecosystem CO_2 exchange (Peng et al., 2024; Wang et al., 2023). Previous studies have shown that the decline of the carbon sink in tropical forests for decades has mainly been attributed to the increased tree mortality rate caused by high temperatures and extreme water conditions in the Amazonian rainforest (Hubau et al., 2020), corroborating former research indicating a negative correlation between net primary productivity (NPP) and mean annual temperature, as well as annual precipitation, in humid tropical forests (Schuur, 2003). The increase in atmospheric vapor pressure deficit under water stress was also believed to limit the productivity of tropical forests by reducing stomatal conductance, thereby reducing transpiration and photosynthesis, leading to a decrease in carbon uptake (Chayawat et al., 2019; Law et al., 2001). In addition, radiation was considered an important factor in controlling plant photosynthetic activity in tropical forests through radiative transfer in the forest canopy, and it also has the possibility to influence forest carbon uptake by influencing canopy structure (Aguilos et al., 2018; Wolf et al., 2011). Large and intact primary tropical rainforests are distributed in Xishuangbanna, southwestern China, which are on the northern edge of tropical Asia and have developed under conditions of relatively lesser precipitation and lower temperatures than the central area of tropical Asia (Zhu et al., 1998). Influenced by the Indian monsoon, climate seasonality shapes the species composition, community structure, and phenology of our study rainforest, which is therefore classified as a tropical seasonal rainforest (Zhu, 1992). Previous studies based on eddy covariance observation have proved the protected primary rainforest in Xishuangbanna to be a weak carbon sink with an annual mean value of 125 g C m^{-2} $year^{-1}$, and the carbon dynamic showed strong seasonality and low carbon use efficiency due to strong respiration during the rainy season (Tan et al., 2010; Yao et al., 2012; Zhang et al., 2006b). Due to the special location, which lies in the transition zone between tropical and sub-tropical regions, this tropical seasonal rainforest is highly susceptible to critical transitions and acts as an amplifier of disturbances (Seddon et al., 2016; Scheffer et al., 2009), making it sensitive to changes in biophysical factors. Therefore, the CO_2 exchange dynamic in the rainforests of Xishuangbanna largely reflect the sensitivity of tropical and sub-tropical forest response to global change. For the protected primary rainforest in Xishuangbanna, temperature conditions were more important than water conditions in affecting its carbon sink at the annual scale (Fei et al., 2018). At the seasonal scale, a distinct seasonal carbon exchange pattern occurred because of the strong seasonality of ecosystem respiration (Reco), which was associated with the local phenology of "intensive leaf change" (upper layer canopy (30–40 m) defoliation (March–April) and leaf flushing (May)) and the changes in environmental conditions (Tan et al., 2014; Zhang et al., 2010). The long-term trend of CO_2 exchange of the Xishuangbanna primary tropical rainforest and its driving forces have been scarcely reported.

Regarding the inadequate knowledge of the long-term CO_2 exchange dynamic due to the lack of in-situ observations, this study analyzed the 20-year CO_2 flux data based on the eddy covariance (EC) technique and evaluated the impact of biophysical drivers (meteorological and physiological indicators) on CO_2 flux exchanges in the northern edge of tropical Asia in the Xishuangbanna tropical rainforest ecosystem. For this well-protected seasonal rainforest without disturbance from human activity, which was previously reported as a weak carbon sink (Zhang et al., 2006b) based on two-year EC observations, we hypothesize that (1) there is a stable or even increasing trend of inter-annual carbon sink during the two decades; (2) CO_2 exchange during the rainy and dry seasons is regulated by biophysical drivers that have varied over the past two decades. Among them, temperature has been shown to affect NEP (Fei et al., 2018) significantly, motivating our hypothesis that it also regulates its inter-annual trend.

2. Materials and methods

2.1. Study site

The study site is located in a tropical seasonal rainforest natural reserve in Xishuangbanna, southwestern China (21°55′39″N, 101°15′55″E, elevation 750 m) (Fig. 1). Affected by the Indian monsoon, this area has a rainy (May–October) and a dry (November–April) season. The dry season of this seasonal rainforest is dominated by two subseasons, the early stage is the foggy–cool period from November to February of the following year, with the average number of monthly foggy days exceeding 23 days (Zhang et al., 2018). During the foggy–cool period, fog events usually occur in the second half of the night (0–6 am) and completely dissipate around 11 am, with a maximum daily duration of 10.5 h (Zhang et al., 2018). Fog water also contributes to precipitation inputs in this period. The annual average and average daily fog drip was 89.4 ± 13.5 mm (mean ± 1 SD) and 0.38 ± 0.27 mm d^{-1} respectively for all days when fog drip occurred. Fog drip contributes around 5 % of the annual rainfall (Liu et al., 2004). The second stage is the clear period from March to April before the rainy season, when there are usually less moisture and higher temperatures than the foggy–cool period. The clear period is also recognized as “dry-hot” period in previous study (Zhang et al., 2010). The mean annual temperature is 21.2 °C, and the mean annual precipitation is around 1417.7 mm. This forest has a lower soil moisture level compared to other typical tropical rainforests (Kupers et al., 2019; Takamura et al., 2023). The forest is old growth (>180 years) (Yan et al., 2013) and well protected. The mean canopy height ranges from 30 to 35 m with uneven canopy layers, while the mean canopy height and density of trees with a diameter at breast height greater than 10 cm are 35 m and 386 ha^{-1}. This forest is composed by three general tree layers. Layer 1 contains more than 70 % of all individual trees (below 16 m), including small evergreen trees and juveniles of species from the upper tree layers (above 16 m). Layer 2 consists of a mixture of evergreen and deciduous species, such as *Barringtonia macrostachya, Gironniera subaequalis*, and *Sloanea cheliensis* (16−30 m). Layer 3, is dominated by *Pometia tomentosa* and *Terminalia myriocarpa* (over 30 m) (Zhou et al., 2017; Zhang et al., 2006b). The Xishuangbanna ecological observation and research station (site code BNS in FluxNet), built in 2002, has already accumulated 20 years of carbon flux and meteorological data based on the EC system. Such a long time series dataset enables us to explore the long-term dynamics of the tropical forest carbon sink and its biophysical regulation mechanisms (Baldocchi, 2020).

2.2. Data collection and processing

2.2.1. Meteorological data and flux data

A flux tower was set up at a height of 74 m on a permanent sample plot of 1 ha in the tropical seasonal rainforest natural reserve with the EC flux system (at 48.8 m, based on an average canopy height of 32.5 m) and the routine meteorological measurement system (RMMS) installed. The study plot is located in a typical valley for tropical seasonal rain forest (Zhang et al., 2010; Tan et al., 2010), which covers a flat area approximately 40 m wide between two hills extending from east to west. The slopes to the south and north of the site are about 20° The length of the valley is about 2 km. The EC flux system consists of a 3D sonic anemometer (CSAT3, Campbell, USA) and an open-path infrared gas analyzer (Li-7500, Li-Cor, USA). The eddy flux footprint ranges from 50 m to 350 m in the upwind direction, and the average range

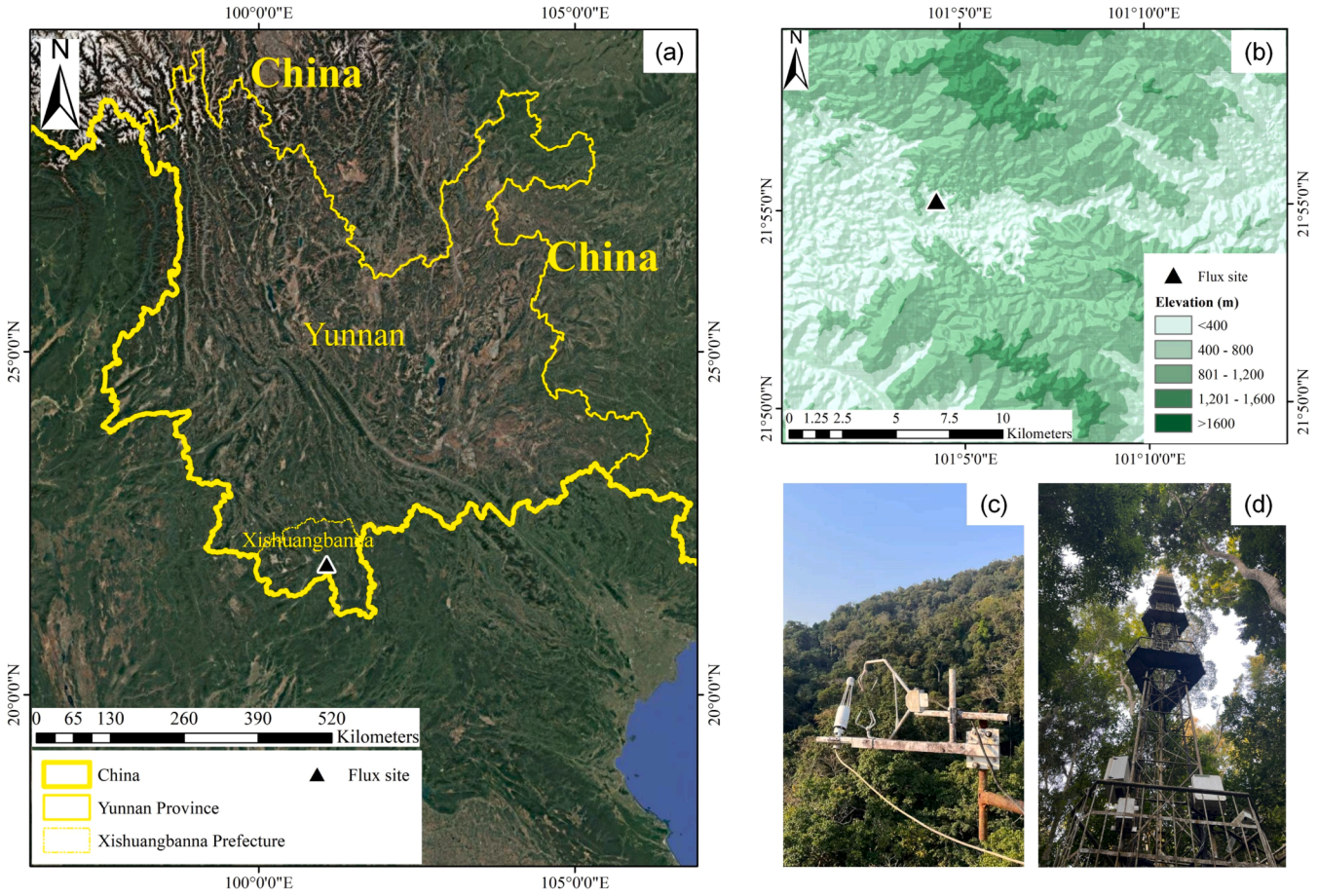

Fig. 1. (a) Geographical location of Xishuangbanna seasonal rainforest natural reserve, (b) topographical features around the flux tower, (c) the eddy covariance (EC) flux system, and (d) flux tower.

perpendicular to the main wind direction is between −100 m and 100 m. The fetch can satisfy the request of footprint and more than 70 percent fluxes comes from the seasonal rainforest ecosystem that we concern (Zhang, 2009; Mi et al., 2006). Our preliminary research has proved that the power spectra and co-spectra in our site obeyed the −2/3 and −4/3 power law by using FFT method (Tan, 2010). The well-developed turbulence and negligible high- and low-frequency flux loss demonstrated by the spectral analysis was also stated in several relating studies of this ecosystem (e.g., Mi et al., 2006; Zhang et al., 2006b; Tan et al., 2010; Li et al., 2010; Yan et al., 2013).

Raw meteorological and flux data were recorded into a data logger (CR1000 and CR5000, Campbell, USA). The CO_2 fluxes were calculated as the covariance between the instantaneous deviation of the gas mixing ratio and the vertical component of wind velocity (Baldocchi, 2003). Seven levels of instruments (at 2.2, 8.7, 16.8, 21.3, 28.9, 37.8, and 56.6 m) were installed on the tower to obtain profiles of wind speed (A100R, Vector Instruments, UK), air temperature (Tair), and relative humidity (RH) (HMP45C, Vaisala, Finland). Vapor pressure deficit (VPD) was calculated using the comprehensive expression of Tair and RH (Monteith and Unsworth, 2013). Instruments for measuring wind direction (W200P, Vector Instruments, UK) and precipitation (P) (Rain Gauge 52203, R. M. Young, USA) were installed at the top of the tower (69.8 m). Solar radiation (Rs) was measured using a pyranometer (CM11, Kipp & Zonen, Netherlands) from heights of 41.6 m and 69.8 m. Photosynthetically active radiation (PAR) was measured using linear sensors (LQS70–10, Apogee, USA) at five heights (3.9, 10.2, 21.0, 31.2, 36.2, 69.7 m). Soil temperature (Tsoil) profiles were monitored at nine depths (0, 5, 10, 15, 20, 40, 60, 80, 100 cm) (105/107 L, Campbell, USA). Soil moisture (Volumetric water content, VWC) profiles were monitored at three depths (5, 20, 40 cm) (CS615-L, Campbell, USA).

Data quality control was performed before using the flux data. After performing spikes exclusion, coordination correction (natural wind system triple rotation method), and WPL (Webb, Peaman, and Leung's calibration method) calibration in EddyPro software (Li-Cor, USA), the flux data with rainfall were excluded. To eliminate the potential advective flux loss due to the complex terrain of this site, the coordinate system rotation for the three-dimensional wind speed was applied according to Tanner and Thurtell (1969) (Li et al., 2010). Nighttime data with friction velocity (u*) below 0.1 $m\ s^{-1}$ were excluded, based on the u* threshold approach (Zhang et al., 2006a), to ensure flux data quality under weak turbulence conditions. Therefore, outlier exclusion and the u* filtering method were applied next (u*<0.1m/s, −60<NEE<45 μmol $m^{-2}\ s^{-1}$), followed by energy closure evaluation and canopy storage flux measurement.

Excluding missing and filtered values, the proportion of effective flux data is approximately 60 % annually, which was 57 % in rainy season and 62 % in dry season. There is an energy balance closure of 70 % at this site. Besides the effect of rainfall, fog droplets severely interfere with the gas analyzer and the sonic anemometer, causing data spikes (Yu et al., 2006). Then, NEE values were gap-filled utilizing the marginal distribution sampling approach and partitioned into Reco (Eq. (2)) and GPP (Eq. (3)) using the nighttime-based algorithm (Reichstein et al., 2005). Online gap filling of flux data, NEE calculation (Eq. (1)), and partition were performed by the REddyProc online tool (https://www.bgc-jena.mpg.de/5622399/REddyProc). Thus, we ensured that the gap-filled data for further analysis were evenly distributed across the seasons and representative of typical meteorological and ecological conditions.

Forest net ecosystem carbon exchange (NEE) is the turbulence CO_2 flux (*Fc*) and canopy CO_2 storage (*Fs*) observed in EC systems.

$$NEE = F_C + F_S = \rho\overline{w'c'} + \frac{\Delta c}{\Delta t} z_r \quad (1)$$

where F_c represents the turbulent eddy flux exchanged between the atmosphere and the measurement height (z_r) of the EC system (48.8 m) while F_s denotes the storage flux in the air layer below the measurement height. F_s was estimated from the rate of change in CO_2 concentration at the EC measurement height over each 30-minute interval, assuming a well-mixed canopy layer (Zhang et al., 2010). ρ, w, and c stand for air density, vertical wind velocity, and CO_2 concentration fluctuations from the respective means, respectively. The primes indicate deviations from the mean, and the over-bar represents the time-averaged value (30 min in this scenario). Δc refers to the change in concentration over the 30-minute period at height z_r, and Δt denotes the time interval. Negative and positive values of NEE represent the carbon sink and carbon source of the forest ecosystem, respectively.

Ecosystem respiration (Reco) includes nighttime (R_n) and daytime respiration (R_d), as shown in Eq. (2). Due to the lack of photosynthesis that absorbs CO_2 in the ecosystem at night, NEE at night is the value of respiration (R_n). Therefore, the effective data of NEE at night and the concurrent surface soil temperature data were fitted into the Lloyd–Taylor equation (Lloyd and Taylor, 1994) to obtain relevant parameters, and the daytime ecosystem respiration (R_d) was calculated using this equation. Gross primary productivity (GPP) was calculated by the difference between Reco and NEE.

$$Reco = R_n + R_d \quad (2)$$

$$GPP = Reco - NEE \quad (3)$$

The light response curve of vegetation was fitted using the Michaelis–Menten equation (Eq. (4)) to obtain (Falge et al., 2001):

$$NEE = \frac{\alpha \times PAR \times P_{max}}{\alpha \times PAR + P_{max}} - R_d \quad (4)$$

where α represents the apparent quantum yield of the ecosystem, PAR represents photosynthetically active radiation, P_{max} represents the maximum photosynthesis rate, and R_d represents the daytime respiration of the ecosystem.

Light use efficiency (LUE) is applied to evaluate vegetation carbon uptake (Fei et al., 2019) and radiation utilization. Ecosystem LUE was calculated with the ratio of GPP to incident PAR at the ecosystem level (Austin et al., 1978; Gilmanov et al., 2007; Pangle et al., 2009; Shi et al., 2014) (Eq. (5)).

$$LUE = \frac{GPP}{PAR} \quad (5)$$

Water Use Efficiency (WUE) is a key parameter for evaluating the coupling between carbon and water cycles in terrestrial ecosystems. It is commonly defined as the ratio of gross primary productivity (GPP) to evapotranspiration (ET) (Knauer et al., 2017).

$$WUE = \frac{GPP}{ET} \quad (6)$$

The inter-annual standardized precipitation evapotranspiration index (SPEI) based on monthly data was estimated to present the moisture condition each year using Climate Indices (2.0.1) in Python 3.9 (Adams, 2017).

2.2.2. Leaf area index data

To measure the leaf area index (LAI) at the site, we randomly selected four sample points within the 1-ha sample area within the dominant flux contribution zone and conducted repeated measurements on each of them every month from 2005 to 2022. LAI was measured using a canopy analyzer (Model LAI-2200, Li-Cor, USA) around the 25th day of each month. Due to the relatively even sunlight in the morning, measurements were usually recorded in the morning. After acquiring the data, we calculated the mean and standard deviation of LAI over the four plots for each month. Then, we used FV2200 software (Li-Cor, USA) to apply leaf angle distribution to obtain total LAI. From 2003 to 2004, due to a lack of measured LAI data, we downloaded MODIS data (MOD15A2H) for the same measurement date from the website (https://modis.gsfc.nasa.gov/), then processed the image utilizing MRT tools, and extracted the total LAI value using the geographic coordinates of the flux station in ArcGIS Software (Esri, USA).

2.3. Statistical analysis

The value of NEE is negative when the ecosystem is a net carbon sink. To better recognize the positive or negative correlation between biophysical drivers and carbon sink, NEP was estimated as "-NEE" to evaluate the CO_2 exchange in this study. It should be noted that this EC-based NEP (Baldocchi et al., 1988; Aubinet et al., 1999) did not incorporates carbon losses from advection, erosion, and aquatic export. Given the widespread use of the Mann–Kendall test and Sen's slope test in time series analysis (Chen et al., 2016), we employed the 'trend' package in RStudio 4.1.1 to analyze long-term trends in biophysical factors (including meteorological data, LAI, and CO_2 concentration data) and flux data (NEP, Reco, GPP). This approach allowed us to calculate the significance of linear trends and determine the annual average rate of change (slope/mean value). To understand the impact of biophysical factors on the carbon sinks over 20 years, we performed convergent cross-mapping (CCM) (Sugihara et al., 2012) using the R package 'rEDM'. The CCM method is a non-parametric method based on empirical dynamics and Takens' theorem to capture causal relationships in complex ecosystems (Sugihara et al., 2012; Ye et al., 2015). Cross Map Skill (ρ) indicates the Pearson correlation coefficient between NEP predicted by various biophysical factors and observed NEP. An increase in ρ with time series length indicates a causal relationship between the factor and NEP. The Fisher' Z test and Kendall's τ test were performed to test the significance of the causal relationships (Chang et al., 2017). Since the CCM analysis was conducted using monthly-scale biophysical data and NEP, the results primarily capture the seasonal influences of biophysical factors on NEP. As the time series length increases, the analysis incorporates longer-term variations, allowing for insights into both seasonal and inter-annual dynamics. Moving window correlation analysis was applied utilizing the 'TTR' R package and the results were visualized with the 'pheatmap' R package to examine the long-term correlation between biophysical factors and NEP in different seasons. To minimize the influence of seasonal patterns and highlight the inter-annual effects, a 12-month window size was used. All statistical figures were created using Origin 2023b (OriginLab, USA).

3. Results

3.1. Seasonal variation and long-term dynamics of biophysical factors

The biophysical factors in our site from 2003 to 2022 exhibited consistent seasonal and inter-annual patterns (Fig. 2). Tair and Tsoil rose from the start of the year, peaked in June, and declined afterward (Fig. 2 (a)). Tsoil lagged slightly behind Tair, with ranges of 15.9–23.5 °C and 16.0–24.3 °C, respectively. Daily Tair differences were highest in March (14.5 °C) and lowest in July (5.2 °C). P decreased early in the year, reaching a low in February (23.7 mm), then increased sharply after May, peaking in July (309.6 mm) (Fig. 2(b)). VWC mirrored P, ranging from 0.16 to 0.27 m^3 m^{-3}. which is lower than some lowland tropical rainforests (Aguilos et al., 2018; Kosugi et al., 2012). VPD peaked in April (0.68 kPa) during warm, dry conditions (Fig. 2(c)). PAR and Rs followed similar patterns, peaking in April (522.9 MJ m^{-2} $month^{-1}$ and 745.2 mol m^{-2} $month^{-1}$) (Fig. 2(d)). LAI decreased early in the year, reaching a low in April (4.90 m^2 m^{-2}), before recovering to a peak around October

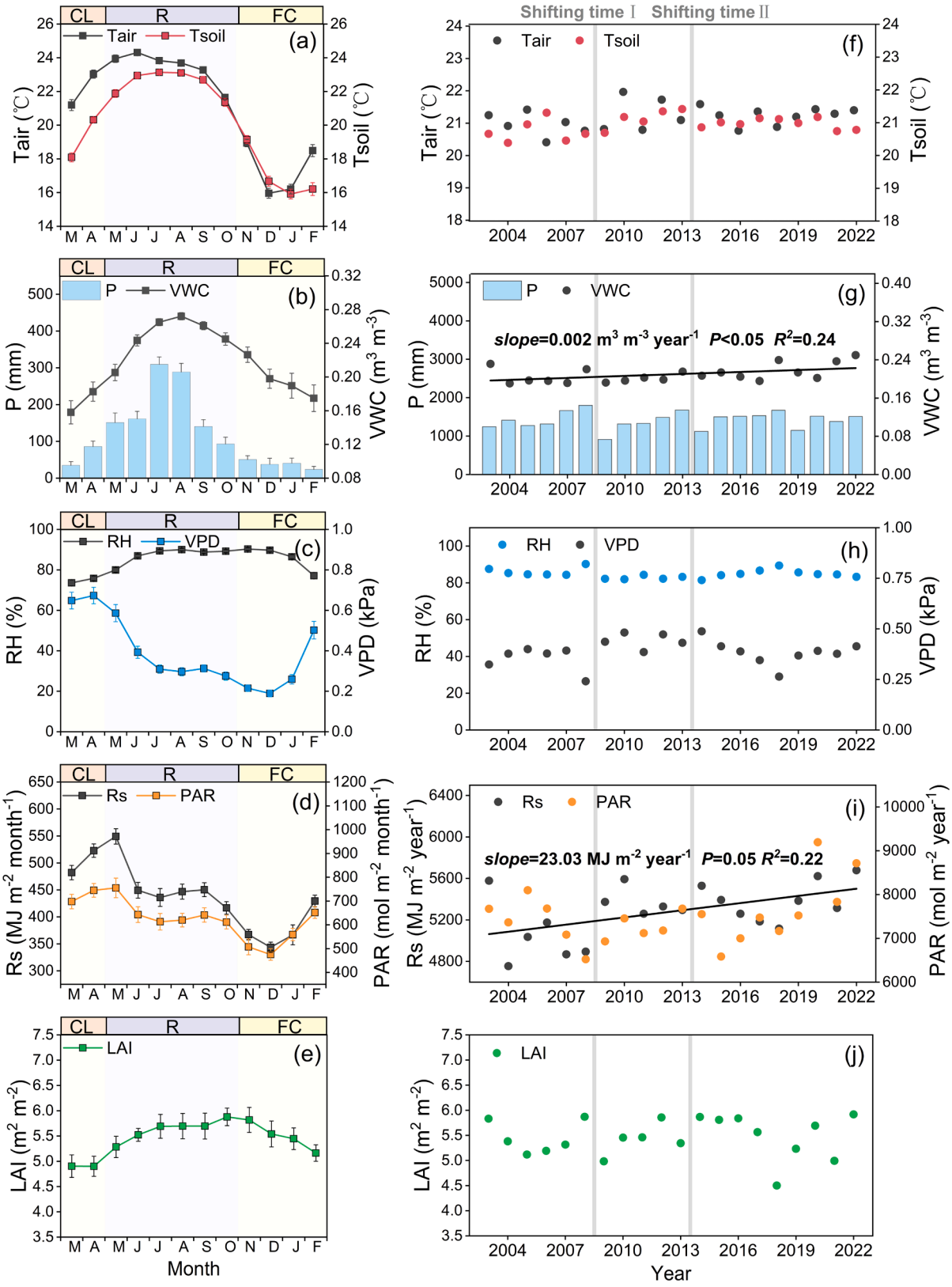

Fig. 2. (a)–(d): Temporal variation in monthly mean air temperature (Tair) and soil temperature (Tsoil); mean precipitation (P) and volumetric water content (VWC); mean relative humidity (RH) and vapor pressure deficit (VPD); and cumulative solar radiation (Rs) and photosynthetically active radiation (PAR); (e)–(j): Temporal variation in annual mean air temperature (Tair) and soil temperature (Tsoil), mean precipitation (P) and volumetric water content (VWC), mean relative humidity (RH) and vapor pressure deficit (VPD) and cumulative solar radiation (Rs) and photosynthetically active radiation (PAR). "CL", "R" and "FC" indicate clear period of dry season, rainy season and foggy–cool period of dry season respectively. Error bars indicate the interannual standard errors of monthly values for each factor. The solid line represents the significant trend. Vertical grey lines mark the shifting time from wet to dry conditions based on SPEI.

(5.8 m^2 m^{-2}) (Fig. 2(e)).

During the rainy season, favorable temperatures (Tair = 23.4 °C, Tsoil = 22.9 °C) (Fig. 2(a)) and moisture (P = 190.7 mm $month^{-1}$) supported maximum LAI (5.6 m^2 m^{-2}) (Fig. 2(b), 2(e)). The foggy–cool period of dry season had lower temperatures (Tair = 17.4 °C, Tsoil = 18.7 °C), scarce precipitation (P = 38.1 mm $month^{-1}$), and stable moisture (VPD = 0.29 kPa, VWC = 0.19 m^3 m^{-3}) (Fig. 2(a), 2(b), 2(c)). The clear period of the dry season was characterized by relatively low precipitation (P = 60.4 mm $month^{-1}$), strong solar radiation (Rs = 502.6 MJ m^{-2} $month^{-1}$, PAR = 720.6 mol m^{-2} $month^{-1}$), and moderate air and soil temperatures (Tair = 22.1 °C, Tsoil = 19.5 °C) (Fig. 2(a), 2(b), 2(d)). This period also coincided with the lowest LAI (4.9 m^2 m^{-2}), primarily due to seasonal leaf shedding in the upper canopy (Fig. 2(e)).

Inter-annual trends were stable over 20 years. Mean annual Tair and Tsoil were 21.2 °C and 20.1 °C, respectively (Fig. 2(f)), with Tsoil increasing slightly during the rainy season (Slope = 0.03 °C $year^{-1}$) (Figure S1(f)). Mean annual P was 1417.7 mm, with extremes of 913.8 mm (2009) and 1801.1 mm (2008) (Table S1, Fig. 2(g)). Dry season P and VWC increased significantly (Slopes = 10.2 mm $year^{-1}$ and 0.004 m^3 m^{-3} $year^{-1}$), while PAR rose notably (Slope = 3.17 mol m^{-2} $year^{-1}$) (Figure S1(b), S1(d)). LAI averaged 5.46 m^2 m^{-2}, reflecting high vegetation coverage without significant inter-annual variation (Fig. 2(j)).

3.2. Seasonal variation and long-term dynamics of CO_2 exchange

NEP, Reco, and GPP exhibited distinct seasonal patterns (Fig. 3). NEP was positive at the start of the year, declined continuously, turned negative in April, and reached a minimum in June (−8.6 g C m^{-2} $month^{-1}$) before rebounding to positive values by September or October (Fig. 3(a)). The highest monthly mean NEP occurred in December (32.7 g C m^{-2} $month^{-1}$). GPP and Reco followed similar trends, peaking in June (GPP = 294.0 g C m^{-2} $month^{-1}$, Reco = 302.6 g C m^{-2} $month^{-1}$) before declining (Fig. 3(b), 3(c)). From April onward, Reco increased faster than GPP, and after September, Reco declined more rapidly. The dry season NEP (148.3 g C m^{-2} $season^{-1}$) accounted for 93.9 % of annual NEP, significantly exceeding the rainy season NEP (9.6 g C m^{-2} $season^{-1}$, 6.1 %). During the dry season, NEP was higher in the foggy–cool period (58.3 g C m^{-2} $month^{-1}$) than in the clear period (15.8 g C m^{-2} $month^{-1}$).

Over the 20-year period, the ecosystem remained a continuous modest carbon sink, with NEP ranging from 51.0 to 260.5 g C m^{-2} $year^{-1}$ (Table S1). NEP showed a significant upward trend (Slope = 5.30 g C m^{-2} $year^{-1}$, growth rate = 3.4 % $year^{-1}$; Fig. 3(d)). GPP (Slope = 26.95 g C m^{-2} $year^{-1}$, growth rate = 1.0 % $year^{-1}$) and Reco (Slope = 22.08 g C m^{-2} $year^{-1}$, growth rate = 0.9 % $year^{-1}$) also increased significantly (Fig. 3(e), 3(f)). Maximum GPP and Reco values occurred in 2021 (3074.8 and 2803.5 g C m^{-2} $year^{-1}$, respectively), while minimum values were in 2008 (2052.6 and 2146.4 g C m^{-2} $year^{-1}$, respectively). Annual mean NEP, Reco, and GPP were 157.9, 2500.2, and 2658.1 g C m^{-2} $year^{-1}$, respectively.

Both GPP and Reco increased during the rainy and dry seasons (Fig. 3). Dry season GPP increased significantly (Slope = 12.34 g C m^{-2} $year^{-1}$, growth rate = 1.2 % $year^{-1}$; Fig. 3h), while Reco showed insignificant growth (Slope = 8.69 g C m^{-2} $year^{-1}$, growth rate = 1.0 % $year^{-1}$; Fig. 3(i)), leading to substantial NEP accumulation (Slope = 3.55 g C m^{-2} $year^{-1}$, growth rate = 2.4 % $year^{-1}$; Fig. 3(g)). During the rainy season, GPP (Slope = 16.01 g C m^{-2} $year^{-1}$, growth rate = 1.0 % $year^{-1}$) increased slightly more than Reco (Slope = 11.25 g C m^{-2} $year^{-1}$, growth rate = 0.7 % $year^{-1}$; Fig. 3(k), 3(l)), resulting in modest NEP

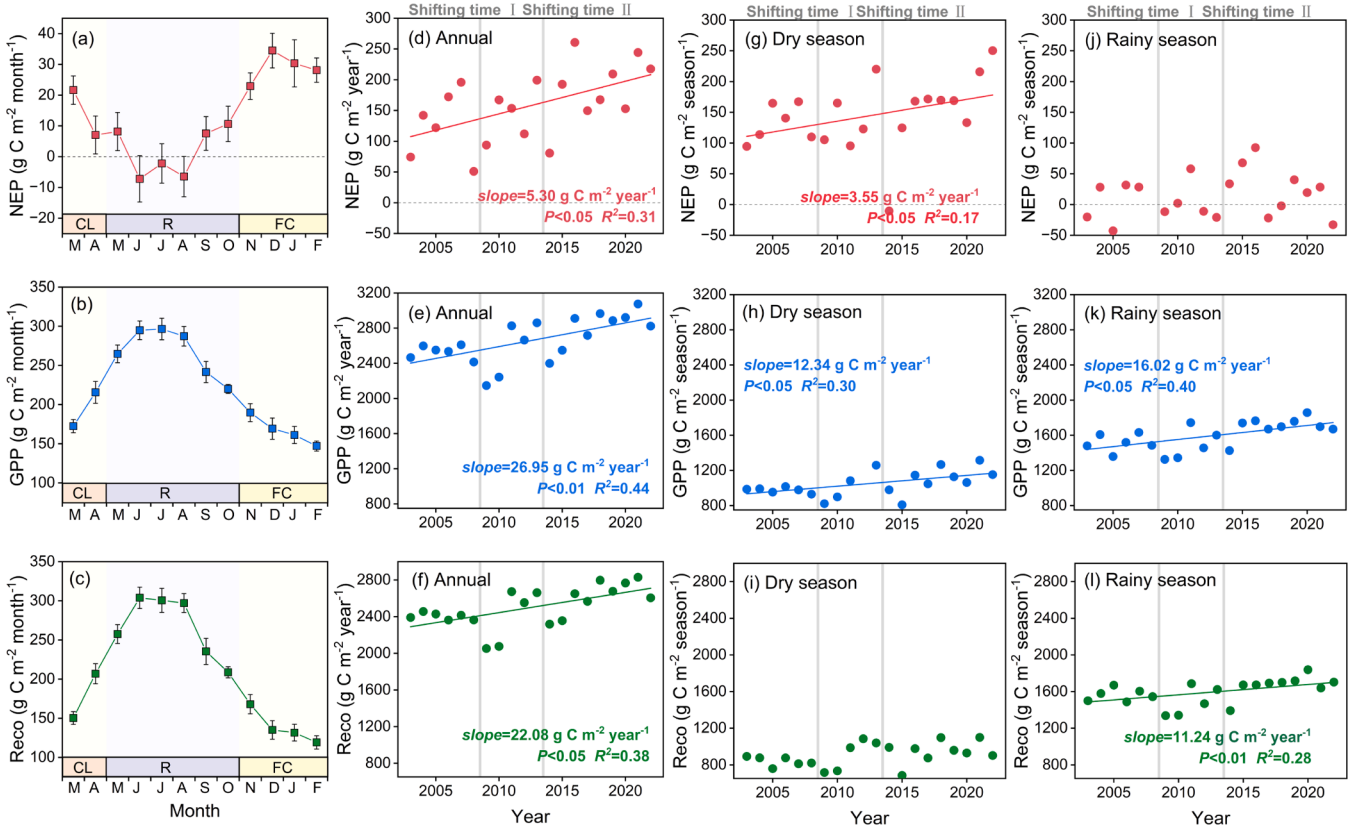

Fig. 3. Temporal variation in monthly (a) NEP, (b) GPP, and (c) Reco, annual (d) NEP, (e) GPP, and (f) Reco, dry season (g) NEP, (h) GPP, and (i) Reco, rainy season (j) NEP, (k) GPP, and (l) Reco from 2003 to 2022. The solid lines denote significant trends, the dashed lines denote insignificant trends. "CL", "R" and "FC" indicate clear period of dry season, rainy season and foggy–cool period of dry season respectively. Vertical grey lines mark the shifting time from wet to dry conditions based on SPEI.

accumulation (Slope = 1.32 g C m^{-2} $year^{-1}$, growth rate = 4.5 % $year^{-1}$; Fig. 3(j)).

3.3. Long-term correlation between biophysical factors and CO_2 fluxes

Convergence cross-mapping revealed that temperature (Tair and Tsoil) had the strongest and most robust impacts on NEP over the 20-year period, consistent with previous findings (Fei et al., 2018). In contrast, radiation (Rs and PAR) had minimal direct effects (low ρ values), though these may reflect cumulative or long-term processes (high slopes) (Fig. 4(a)). Moving window correlation analysis showed that none of the biophysical factors consistently exhibited either positive or negative correlations with NEP over the 20 years (Fig. 4(b), 4(c)). Notably, between 2009 and 2016, several factors, including temperature, moisture, and radiation, shifted to reversed correlation coefficients in both seasons. In the dry season, most factors (except LAI and VWC) showed no significant positive correlation with NEP before 2013. From 2014 to 2016, temperature (Tair and Tsoil) and radiation (Rs and PAR) exhibited positive or slightly negative correlations with NEP. After 2016, temperature and radiation factors again showed negative correlations with NEP. LAI had a significant positive correlation with NEP before 2013 but showed non-significant or negative influences afterward. In the rainy season, VPD and radiation (Rs and PAR) displayed strong positive correlations with NEP in most years. However, this relationship shifts to a negative correlation in one or two years after 2009 and 2014. During this period, rainfall and VWC exhibited slight opposite trends to radiation factors. Over the 20 years, VPD and radiation maintained the most stable correlations with NEP in the dry season, while LAI showed a stable correlation in the rainy season. These shifts in driver–NEP correlations typically occurred 2–3 years after the transitions from wet to dry conditions (2009 and 2014) (Figure S2).

GPP generally increased with higher PAR, Tair, and VWC (Fig. 5(a), 5(b), 5(c); Table S2). The slope of the linear correlation between PAR and GPP reflects changes in ecosystem light use efficiency (LUE), which ranged from 0.2 to 0.4, with higher LUE in the rainy season compared to the dry season (Fig. 5(a)). The effect of Tair on GPP varied across periods, but higher temperatures generally corresponded to larger GPP. Lower Tair in earlier years was associated with smaller GPP during the rainy season and the foggy–cool period of the dry season. Similarly, lower VWC in earlier years coincided with reduced GPP in these periods. GPP increased with VPD during the foggy–cool period but decreased with VPD in the rainy season and clear period. However, the rainy season reached peak GPP within the same VPD range as the foggy–cool period. Additionally, the rainy season achieved higher GPP than the foggy–cool period at similar LAI levels. In most years, the clear period had lower LAI than the foggy–cool period but maintained comparable GPP levels.

Reco increased with stable or rising Tsoil and VWC throughout the year (Fig. 6(a), 6(b); Table S2). Although Reco was estimated from nighttime data using a Q_{10} model (Fang and Moncrieff, 2001; Reichstein et al., 2005), its seasonal and temperature-driven responses were examined across varying temperature ranges, and agree with soil chamber patterns, supporting the Q_{10}-based estimates (Goldberg et al., 2017; Zhang et al., 2015). Unlike the clear period, both Tsoil and Reco increased consistently over the 20 years during the foggy–cool seasons. Earlier foggy–cool seasons had lower Tsoil and smaller Reco compared to later years. The clear and rainy seasons generally exhibited higher Reco than the foggy–cool period in relation to VWC. The positive effect of VWC on Reco was most pronounced in the foggy–cool period (Table S2). The linear correlation between LAI and Reco was weak. At similar LAI levels, the rainy season and clear period had higher Reco than the foggy–cool period (Fig. 6(c)).

4. Discussion

4.1. Small, stable carbon sink during the rainy season

Different from the dry season, which always presented a non-negligible carbon sink, this forest sometimes behaved as a carbon source during the rainy season. The average NEP during the 20 years was only approximately 1.3 g C m^{-2} $month^{-1}$ during the rainy season. Annual rainfall and Tair peaked during the rainy season, with GPP and Reco reaching their maximums throughout the year in the rainy season (Fig. 3). The synchronous levels and slight trends in GPP and Reco during the rainy season over a 20-year period (Fig. 3(k), 3(l)) led to an insignificant increasing or decreasing trend of NEP (Fig. 3(j)). Thus, a

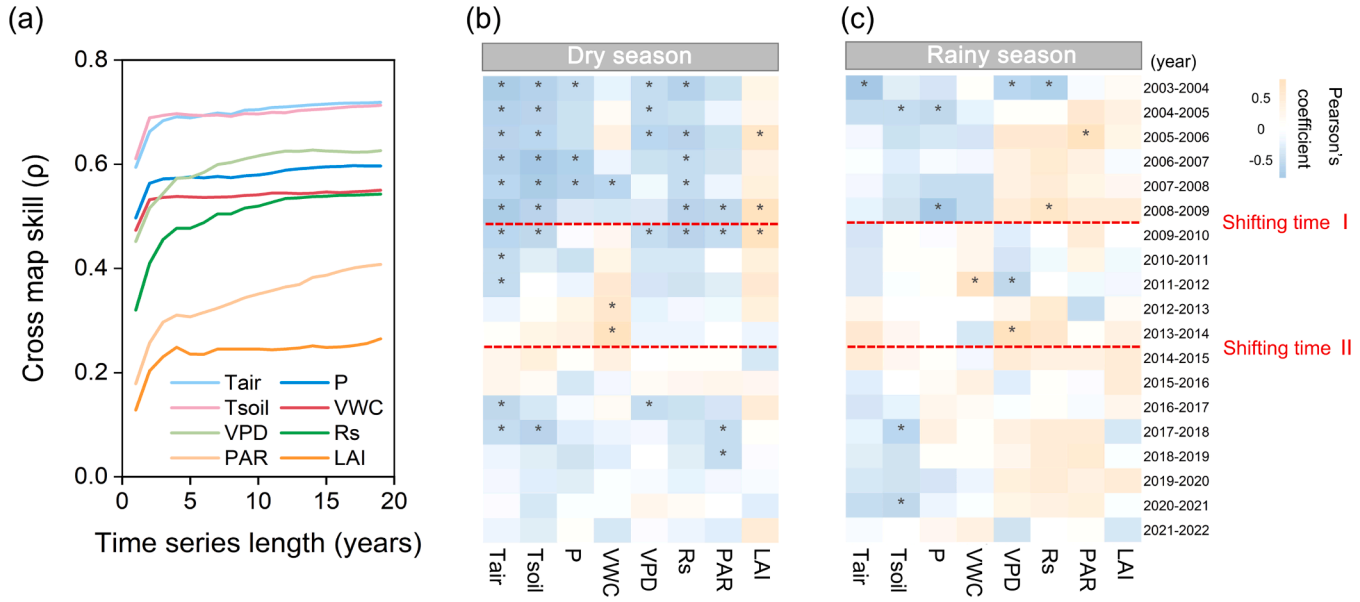

Fig. 4. Long-term correlation between biophysical factors and NEP. (a): Convergent cross-mapping analysis of biophysical forcing impacts on NEP from 2003 to 2022. The correlation (cross map skill, ρ) between predicted and observed NEP strengthens with time series length, gradually stabilizing around 2007 (convergence), indicating the causal relationships between biophysical factors and NEP. (b)-(c): Moving window correlation analysis between biophysical factors and NEP during the dry season and rainy season. * indicates significant correlation ($p < 0.05$). Red lines mark the shifting time from wet to dry conditions based on SPEI. Blue and orange colors represent negative and positive Pearson correlation coefficients, respectively, with color intensity indicating correlation strength.

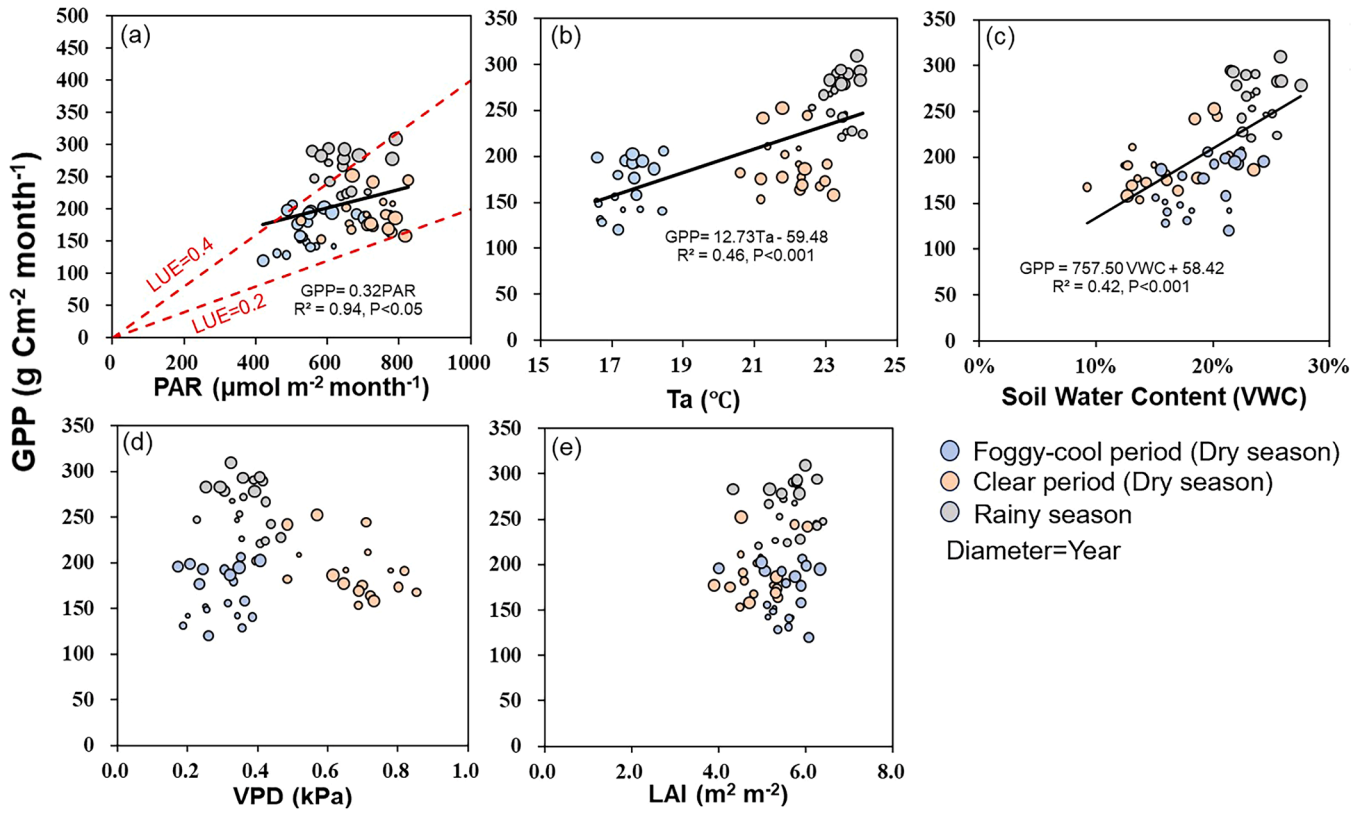

Fig. 5. Correlation between monthly average biophysical factors and GPP in the foggy–cool period and clear period in the dry season, as well as during the rainy season. Each dot represents the monthly average in the different seasons of each year. Dot diameter indicates the year (the smallest one is 2003 while the largest one is 2022). The regressions are based on all season data.

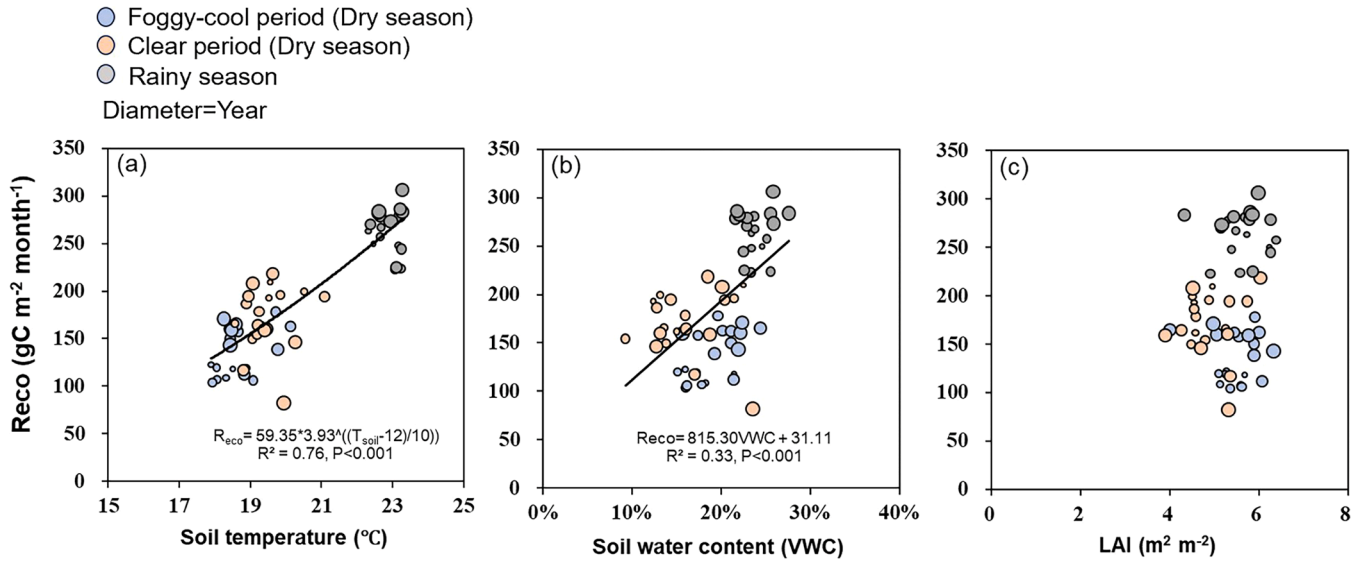

Fig. 6. Correlation between monthly average biophysical factors and Reco in the foggy–cool period and clear period in the dry season, as well as during the rainy season. Each dot represents the monthly average in the different seasons of each year. Dot diameter indicates the year (the smallest one is 2003 while the largest one is 2022). The regressions are based on all season data.

mostly balanced CO_2 exchange between the ecosystem and the atmosphere can be maintained during the rainy season during the 20 years.

This rainy season CO_2 flux pattern is similar to tropical forests in SEA (Saigusa et al., 2008). During the rainy season, tropical seasonal rainforest vegetation exhibited vigorous growth due to elevated temperatures and high moisture availability (Fei et al., 2018; Raich et al., 2006). This growth was further evidenced by the increase in LAI during the rainy season (Fig. 2(e)), which consequently enhanced GPP. The temperature and water conditions of the rainy season may concurrently also increase Reco by enhancing soil enzyme activity and promoting litterfall decomposition (Hikosaka et al., 2006; Zhang et al., 2006b). VPD, Rs, and PAR showed positive correlations with rainy season NEP (Fig. 4(c)), except for the one or two years after 2009 and 2014, when a temporary temperature peak was observed (Fig. 2(f)). The high temperature

coupled with reduced precipitation in 2010 and 2014 led to higher VPD and radiation in the rainy season than during the other years and resulted in a depression in NEP. This is also the reason why the correlation between precipitation and NEP showed a moderate increase after 2013, when the annual precipitation input largely grew and mitigated the stress of high VPD and radiation on photosynthesis. In approximately two years following 2009 and 2014, which are periods characterized by lower precipitation and warmer temperatures, the NEP transitioned from a carbon source to a carbon sink during the rainy season (Fig. 3(j)). This shift may be attributed to a reduction in ecosystem respiration driven by decreased precipitation and VWC, which outweighed the limitation effects high radiation and VPD on photosynthesis. Precipitation and soil moisture changed insignificantly during the rainy season, hence their effect on GPP and Reco was limited during the 20 years.

4.2. Significant role of carbon sinks during the dry season

Dry season NEP accounted for 93.9 % of the annual mean NEP. The mean GPP was 167.3 and 191.1 g C m^{-2} $month^{-1}$, and the mean Reco was 138.3 and 176.1 g C m^{-2} $month^{-1}$ in the foggy–cool and clear periods, respectively, during the 20 years. Despite the larger GPP in the clear period than in the foggy–cool period, the foggy–cool period carbon sink basically accounted for over 60 % of the carbon sink during the dry season except in 2013, 2015, and 2021, with a 20-year mean NEP of 29.2 g C m^{-2} $month^{-1}$, while the 20-year mean NEP for the clear period was 15.8 g C m^{-2} $month^{-1}$ (Fig. 3). As suggested by Fig. 6(c), LAI remained low for more than 10 years only in the clear periods; for the same year, Reco levels in the clear period were scarcely less than in the foggy–cool period. The "intensive leaf change" phenomenon (suggested by the low LAI during the clear period, Fig. 2(e), Figure S3) resulted in great accumulation of litterfall and in the large Reco at this period (Zhang et al., 2006b; Zheng et al., 2005). This result suggests that the biophysical conditions of the foggy–cool period were more beneficial for carbon accumulation (Fig. 5(a)). Hence, the larger contribution of the foggy–cool period to the dry season carbon sink was not only caused by its longer time occupation (four months) per year compared with clear period (two months) but was also largely decided by the higher CO_2 uptake capacity. The trend analysis results show that the increase in NEP occurred significantly during the dry season (Fig. 3(d)). The faster inter-annual growth rate of GPP compared with Reco had led to the accumulation of NEP during the dry season over time (Fig. 3(h), 3(i)).

Insolation was considered the main factor affecting the dry season CO_2 uptake in tropical rainforests (Zhang et al., 2010). The foggy–cool period had lower radiation (Fig. 2(d)) due to the frequent occurrence of fog. The increasing LUE with the improved range of PAR can be found during the foggy–cool periods of the two decades (Fig. 5(a)). Especially LUE improvement (Figure S4(a)) during 2013 to 2016 corresponded well to the positive correlation coefficient between PAR and NEP during the dry season (Fig. 4(b)). The PAR level was getting close to the clear period and rainy season levels (Fig. 5(a)), leading to larger GPP compared with the early years. This increasing PAR in the foggy–cool period may be associated with reduced cloud cover and radiation fog levels, potentially caused by deforestation (mainly converting rainforest to rubber plantation) (Cheng and Xie, 2008; Liu et al., 2003; Qi et al., 2014; Zhang et al., 2014) in Xishuangbanna (prefecture) region. This localized phenomenon also aligns with the broader positive trend in solar radiation observed across Southwest China (Jin et al., 2022; Wang et al., 2021). The promoting effect of PAR on NEP occurred with PAR values below approximately 2423.5 mol m^{-2} $period^{-1}$ (Figure S4(b)). Despite PAR showing a slight increasing trend during the 20 years, its fluctuations during foggy–cool seasons have mostly remained under this threshold, primarily enhancing NEP in this period. Especially, along with the reduction of fog in this region, the PAR availability increased, which is beneficial to expand the promoting effect of PAR on NEP. The light-curve analysis (Figure S4(c), Table S3) suggests that the increase in LUE during the clear period was primarily driven by the enhanced radiation conditions. Also, the forest had the highest LAI during this period and notable diffuse radiation due to fog, which has been shown to enhance photosynthesis and GPP, and thereby contributing to higher NEP in the foggy–cool period (Rap et al., 2015; Rodrigues et al., 2024).

We also note that the elevated atmospheric CO_2 concentration during the recent decades has been linked to the increasing carbon sink trend in the tropical forest region (Lewis et al., 2004a, 2004b; Ruehr et al., 2023; Figure S6(a)) due to the CO_2 fertilization effect (Bala et al., 2006; Tharammal et al., 2019). Elevated CO_2 concentrations can enhance ecosystem LUE through several mechanisms, including stimulating photosynthetic carbon gain (Leakey et al., 2009), reducing photoinhibition (Tomimatsu et al., 2014) and influencing chlorophyll synthesis (Singh and Agrawal, 2015). A larger ecosystem LUE can be achieved with a lower contribution of Rubp-limited photosynthesis and a larger contribution of Rubisco-limited photosynthesis. Moreover, the observed increase in water use efficiency (WUE) further supports our inference that elevated CO_2 and radiation jointly enhanced GPP, leading to disproportionate gains in carbon assimilation relative to evapotranspiration—consistent with global WUE trends under rising CO_2 (Figure S8; Zhang et al., 2022; Walker et al., 2021). Such a mechanism requires further detailed investigation and analysis of the specific physiological process. Nevertheless, our results strongly proved the stimulating effect of increasing PAR on GPP and the long-term carbon sink for this rainforest at the ecosystem level.

Water limitation during the dry season severely restricts canopy carbon uptake in tropical forests (Lee et al., 2013; Morton et al., 2014; Restrepo-Coupe et al., 2013; Saleska et al., 2003). The clear period suffers more from drought stress due to its higher temperature and radiation than the foggy–cool period (Fig. 2(a), (d)). Despite the two sub-seasons of dry season had similar extent of precipitation and soil moisture (Fig. 2(b)), the stable and notable carbon sink in the dry season can partly be attributed to the differing sensitivities of the foggy–cool and clear periods to the precipitation input change. During the 20 years, the foggy–cool period has generally maintained a larger NEP than the clear period has. But its NEP displayed a non-negligible decline in 2014 and 2015, when the foggy–cool season showed declined precipitation partitioning (Fig. 7(a)). But for the clear period, a significantly enhanced NEP (even larger than the early years NEP of the foggy–cool periods) appeared in 2015 after the large precipitation partitioning to this period in 2014. Similar regulation can also be found in 2021 (Fig. 7(b)), which may have resulted from the growth in vegetation (LAI) with the increased precipitation input that mitigates the high temperature in the clear period (Figure S5, Ma et al., 2023). Different from the situation in 2015, NEP in 2021 also had a decreased contribution to the whole dry season NEP, as shown by the percentage, but it remained at a stable level. Therefore, decreased precipitation in the dry season may impair the foggy–cool NEP, but this part can well be compensated if dry season rainfall partitioning to the clear period was increased. Enhanced NEP was also reported in other SEA rainforests under La Niña- induced moist conditions, frequently occurring after El Niño events (Takamura et al., 2023). The increased precipitation during the clear period over the years (from around 2009 to 2018) not only allowed LAI to recover and promoted NEP but the simultaneously slight decrease of VPD caused by the increase in precipitation can promote NEP through increased stomatal conductance, which enhanced the process of CO_2 uptake through leaf photosynthesis (Chayawat et al., 2019; Kwon et al., 2008; Law et al., 2001) (Figure S5(a), S5(b)). However, some years had comparatively high LAI but with VPD- or VWC-restricted low NEP (Figure S5(c), S5(d)). Excessive VPD during the dry season will cause stomatal closure to prevent excessive water loss, inhibiting plant growth and, in severe cases, leading to leaf and branch loss (Yan et al., 2016). In the early years, mean VPD during the clear period exceeded 0.6 kPa. Beyond this threshold, NEP usually decreases with a VPD increase (Figure S5(c)). Besides the effect of atmosphere moisture, which is represented by VPD, the increase in soil moisture (VWC) caused by increased precipitation

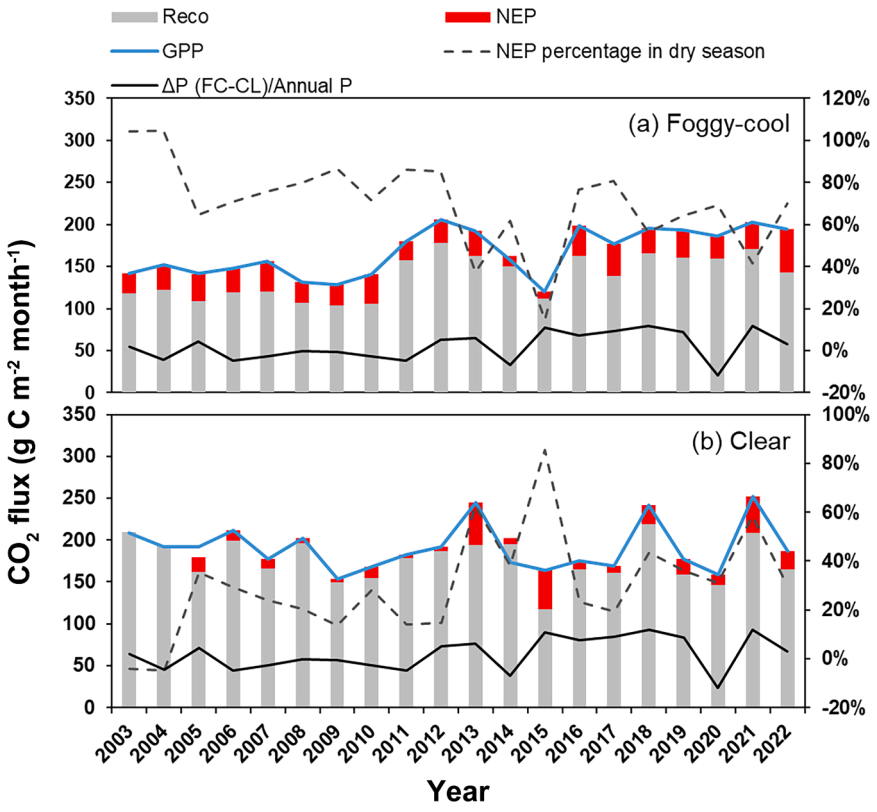

Fig. 7. Variation in the contribution of Reco and GPP to NEP in the dry season accompanied with rainfall partitioning. (a) Foggy–cool period; (b) Clear period. "NEP percentage in dry season" indicates the contribution of foggy–cool or clear period NEP to the whole dry season NEP. "ΔP (FC—Cl)/Annual P" indicate the difference in annual rainfall partitioning to the foggy–cool and clear periods.

also had a positive effect on NEP through photosynthesis in recent years (Figure S6(b)), which was controlled by physiological processes (Martínez-Vilalta et al., 2014; Sohel et al., 2021). This can be evidenced by the sensitive response of GPP to soil moisture across seasons and years (Fig. 5(c) due to the prevalent water stress experienced by vegetation (Xiong et al., 2022). Meanwhile, the increase in dry season precipitation stimulated litterfall decomposition and CO_2 emission, thereby boosting Reco (Jarvis et al., 2007; Parsons et al., 2014; Sayer et al., 2007; Waring and Powers, 2016; Wieder et al., 2009), especially in the clear period when a large amount of litterfall was present (Figure S7). Therefore, the increasing NEP throughout the years was more evident in the foggy–cool period because Reco increasement was slighter than during the clear period.

Table 1
Inter-annual trends of carbon sinks/stocks in tropical forests around the world.

Continent	Region	Vegetation Type	Annual Rainfall (mm)	Trends	Reference
South America	Muti-stations	Tropical forests		Decrease 1985–2015	Hubau et al., 2020
	French Guiana	Tropical humid rainforest	3041	Increase 2007–2009 Decrease 2010–2011	Aguilos et al., 2018
	Brazil	Tropical seasonal rainforest	1872	Increase 2004–2010	Zeri et al., 2014
	Brazil	Tropical seasonal forests	~1600	Decrease 1987–2020	Maia et al., 2020
Africa	Muti-stations	Tropical forests		Increase 1985–2015	Hubau et al., 2020
	Muti-stations	Tropical forests		Increase 1968–2007	Lewis et al., 2009
	All of Africa	Tropical forests		Increase 1901–2002	Ciais et al., 2009
Asia	Xishuangbanna	Tropical seasonal rainforest	1418	Increase 2003–2022	This study
	Malaysia	Tropical humid rainforest	1804	Increase 2003–2010	Kosugi et al., 2012
	Thailand	Dry dipterocarp forest	985	Stable 2013–2017	Sanwangsri et al., 2018

4.3. Implications for the carbon uptake potential of protected tropical rainforests

Over the past two decades, the Xishuangbanna tropical seasonal rainforest significantly enhanced its carbon sink compared to previous measurement before 2010 (Zhang et al., 2010; Zhang et al., 2006b), contrasting with declining or balanced trends in South America but aligning with stable or increasing sinks in Africa and Asia (Table 1). For instance, South American seasonal and humid tropical forests exhibit relatively large carbon sinks, such as 335 g C m^{-2} $year^{-1}$ in French Guiana—a humid forest on the Guiana Shield with a short dry season (Aguilos et al., 2018)—and 500 g C m^{-2} $year^{-1}$ in a more seasonal southwestern Amazonian forest (Zeri et al., 2014), while a semi-deciduous tropical forest in the southern Amazon Basin was found to be nearly carbon-neutral (Vourlitis et al., 2011); while tropical forests in Africa and Asia show weaker carbon uptake (e.g., ~22 g C m^{-2} $year^{-1}$ in Africa (Hubau et al., 2020) and ~21 g C m^{-2} $year^{-1}$ in Malaysia (Kosugi et al., 2012) and 71 g C m^{-2} $year^{-1}$ in Hainan, China (Li et al., 2018). These differences are likely due to variations in altitude, seasonality, and soil nutrient availability (Malhi, 2012). Also, these listed sites usually had a higher soil moisture level than Xishuangbanna. For example, in Paosh in Malaysia, which is a lowland tropical rainforest located in the center of Tropical Asia, the VWC varied around 0.2 to 0.4, and correspondingly there was a larger Reco and GPP over 3000 g C m^{-2} $year^{-1}$ (Kosugi et al., 2008, Kosugi et al., 2012). The generally lower VWC over years at this site compared to the other tropical forests limited the range of dry season Reco and wet season GPP (Fig. 6(b)), which contribute to the larger carbon sink in dry season than rainy season. The dry–season drought stress (a cumulative precipitation of approximately 273.4 mm from November to April) limits carbon uptake, highlighting the ecosystem's sensitivity to precipitation changes (Zhang et al., 2010). Comparing with other dry forests had similar average level of soil moisture, nearly 84 % of CO_2 uptake was achieved during the rainy season in a savanna ecosystem with higher temperature and radiation, which is opposite to our site (Fei et al., 2018); while in a tropical dry dipterocarp forest with similar annual averages of temperature and precipitation also showed the similar declined activities of carbon exchange due to the decreased precipitation and soil moisture as our sites did (Kaewthongrach et al., 2020). Although shifts in dry and rainy season durations were not evident during the study period, future changes in rainfall patterns and rising temperatures could further constrain carbon sink capacity.

The rainforest's carbon use efficiency (CUE) mirrored the seasonal pattern of NEP, peaking in the dry month of December (20.4 %) and reaching its lowest in the rainy month of August (−2.8 %; Fig. 8). This reflects greater carbon retention during the dry season and higher respiratory losses during the rainy season. Over the study period, CUE showed a significant upward trend (annual mean: 5.9 % ± 1.8 %), driven by faster growth in GPP compared to Reco. Concurrent increases in above- and belowground biomass further underscore the ecosystem's potential for carbon accumulation. However, the annual carbon sink declined temporarily around 2 years post-drought (e.g., after 2009 and 2014, Fig. 3(d)), which suggested that even a small long-term decrease in soil moisture (Fig. 2(g) causes a decrease in carbon sequestration in subsequent years. Hence, if there were increasingly severe and frequent droughts in the future, the carbon sequestration function of this forest may be threatened. Recent studies also demonstrated that repeated and severe droughts can lead to significant reductions in forest carbon uptake, increased tree mortality, and shifts in ecosystem respiration patterns, thereby compromising the long-term carbon sink capacity of tropical forests (Feldpausch et al., 2016; O'Connell et al., 2018; van der Molen et al., 2011). Despite regional carbon losses from deforestation, land-use change, and expanding rubber plantations (Achard et al., 2014; Clough et al., 2016; Tan et al., 2010; Yao et al., 2020)—which reduced Xishuangbanna's biomass carbon stock from 212.6 ± 8.7 Tg C in 1976 to 86.9 ± 3.7 Tg C in 2003 (Li et al., 2008)—protected primary forests demonstrate resilience and capacity to enhance carbon sinks under changing environmental conditions.

5. Conclusion

This study applied the EC technique to verify the increasing carbon sink and the related inter-annual and seasonal effect by biophysical factors in a protected primary tropical forest ecosystem in Xishuangbanna, the northern edge of SEA, from 2003 to 2022. Over the 20 years, the tropical seasonal rainforest ecosystem in Xishuangbanna was a continuous carbon sink, with an annual mean NEP of 157.9 ± 56.7 g C m^{-2} $year^{-1}$ (larger than some reported carbon sinks in SEA rainforests). NEP showed a significant upward trend during the study period, with a growth rate of 3.4 % $year^{-1}$. The increase in NEP was caused by a higher growth rate in GPP (1.2 % $year^{-1}$) than in Reco (1.0 % $year^{-1}$). Nevertheless, in the years following drought (in 2009 and 2014, when SPEI was lower than −1), the annual carbon sink slightly declined, as carbon uptake in the rainy season (temporary shifting from source to

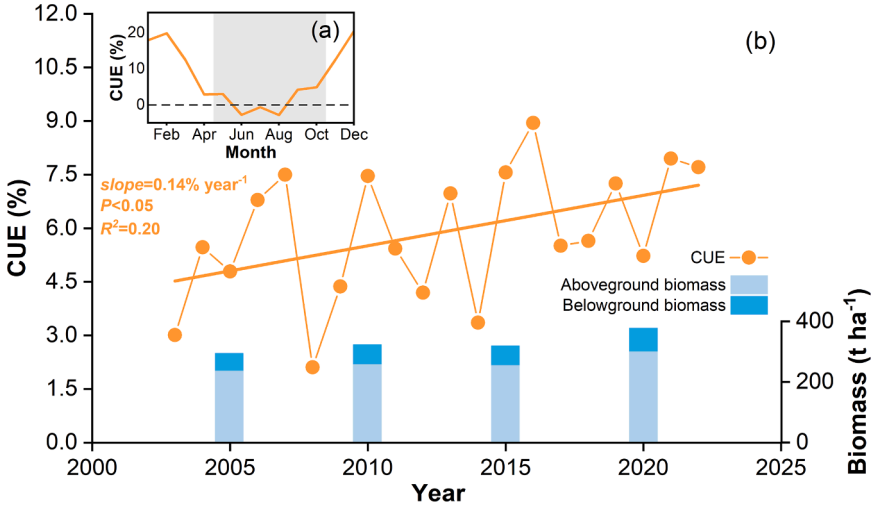

Fig. 8. The carbon use efficiency (CUE) in Xishuangbanna tropical seasonal rainforest. (a) seasonal pattern of CUE and (b) the inter-annual variations in CUE and biomass. CUE was calculated using NEP/GPP (Chen et al., 2019). Biomass data at 5-year intervals were provided by the Xishuangbanna Tropical Rainforest Ecosystem Station (http://bnf.cern.ac.cn/). Estimates were based on tree census data and allometric equations developed from harvested trees across DBH classes. Grey shadow indicates the duration of rainy season.

sink) could not offset the dry season decrease. Agreeing with previous studies, this forest usually presented as a carbon sink in the dry season and as a weak carbon source or a carbon neutral in the rainy season. The CO_2 exchange was dominantly driven by changes in the distinctive factors during the different seasons and sub-seasons. Dry season insolation became higher and water stress was alleviated by more rainfall input, while the rainy season climate remained mostly stable, aside from a minor rise in soil temperature during the 20-year period. The dry season NEP accounted for up to 93.9 % of the annual mean carbon sink and was responsible for the upward trend of the inter-annual carbon sink because the stable temperature and moisture cause the forest to remain largely carbon neutral without distinct fluctuations of the sink or source during the rainy season throughout the 20 years. Enhanced PAR in the moderate range helped this forest maintain an increasing NEP level during the foggy–cool period of the dry season over the years, while the increased precipitation during the clear period over the years is considered the main reason for promoting NEP in the clear period of the dry season. Along with the growth in inter-annual NEP, an increasing CUE based on EC flux and above- and underground biomass can also be found at this site during the two decades, which suggests that the carbon sequestration potential of this forest corresponds to its CO_2 uptake capacity. The positive carbon accumulation trend in Xishuangbanna tropical rainforest resembled that of other tropical forests in SEA and Africa but contrasted with the negative trend in South America. These results indicated the continuous carbon sink potential of the protected tropical rainforests, along with emphasizing the role of rainfall seasonality in regulating the CO_2 exchange in rainforests. Therefore, despite the shifts in the duration of dry and rainy seasons not being evident during the study period, potential changes in the rainfall regime and seasonality, along with the rising temperature in this area should cause concern in the future. Our study highlights the value of a long-term ecosystem CO_2 flux in primary forests at the northern edge of the tropics, which is helpful for improving our understanding of the tropical forest carbon cycle. Future studies still need to build on larger spatial scales and integrate ecosystem process models to better predict ecosystem responses to ongoing climate change.

CRediT authorship contribution statement

Yaqi Liu: Writing – original draft, Visualization, Methodology, Funding acquisition, Data curation, Conceptualization. **Linjie Jiao:** Writing – review & editing, Visualization, Validation, Methodology, Funding acquisition, Data curation, Conceptualization. **Jing Zhang:** Validation, Methodology, Data curation. **Xuefei Li:** Writing – review & editing, Methodology, Funding acquisition, Formal analysis. **Huixu Zheng:** Validation, Methodology, Investigation, Data curation. **Boonsiri Sawasdchai:** Validation, Methodology, Investigation. **Yaoliang Chen:** Writing – review & editing, Validation, Formal analysis. **Yiping Zhang:** Writing – review & editing, Project administration, Data curation. **Palingamoorthy Gnanamoorthy:** Writing – review & editing, Validation, Supervision, Formal analysis. **Qinghai Song:** Writing – review & editing, Supervision, Project administration, Funding acquisition, Conceptualization.

Declaration of competing interest

The authors declare that they have no known competing financial interests or personal relationships that could have appeared to influence the work reported in this paper.

Acknowledgment

We thank Dr. Xuehai Fei, Mr. Donghai Yang, and Ms. Taoxiang Yi for their assistance in the field. This work was supported by the Xishuangbanna Station Tropical Rainforest Ecosystem Research, Chinese Ecosystem Research Networks (CERN), and ChinaFLUX. We appreciate the suggestions by Prof. Timo Vesala from the University of Helsinki, Prof. Yoshiko Kosugi and Dr. Ayaka Sakabe from Kyoto University, and Dr. Satoru Takanashi from FFPRI, Japan.

This study was supported by the National Natural Science Foundation of China (42361144863), International Joint Laboratory of Tropical Asian Forest Carbon Sequestration in Yunnan (202403AP140005), Young Scholars Program of Regional Development, Chinese Academy of Sciences (2022–003), The 14th Five-Year Plan of Xishuangbanna Tropical Botanical Garden, Chinese Academy of Sciences, China Postdoctoral Science Foundation (2024M763515), Yunnan Province "Xingdian Talent Support Program" High-end Foreign Expert Project (E4YNR02B01), the Yunnan Province "Caiyun Postdoctoral Program", China Scholarship Council (No. 202404910056), Finnish National Agency for Education Fellowship (OPH-4675–2024), Research Council of Finland (Mobility Funding 359735).

Supplementary materials

Supplementary material associated with this article can be found, in the online version, at doi:10.1016/j.agrformet.2025.110851.

Data availability

Data will be made available on request.

References

Achard, F., Beuchle, R., Mayaux, P., Stibig, H.J., Bodart, C., Brink, A., Carboni, S., Desclée, B., Donnay, F., Eva, H.D., Lupi, A., Raši, R., Seliger, R., Simonetti, D., 2014. Determination of tropical deforestation rates and related carbon losses from 1990 to 2010. Glob. Chang. Biol. 20, 2540–2554. https://doi.org/10.1111/gcb.12605.

Adams, J., 2017. Climate_indices, an opensource Python library providing reference implementations of commonly used climate indices. https://github.com/monocongo/climate_indices.

Aguilos, M., Hérault, B., Burban, B., Wagner, F., Bonal, D., 2018. What drives long-term variations in carbon flux and balance in a tropical rainforest in French Guiana? Agric. For. Meteorol. 253 (254), 114–123. https://doi.org/10.1016/j.agrformet.2018.02.009.

Aubinet, M., Grelle, A., Ibrom, A., Rannik, Ü., Moncrieff, J., Foken, T., Kowalski, A.S., Martin, P.H., Berbigier, P., Bernhofer, C., Clement, R., Elbers, J., Granier, A., Grünwald, T., Morgenstern, K., Pilegaard, K., Rebmann, C., Snijders, W., Valentini, R., Vesala, T., 1999. Estimates of the annual net carbon and water exchange of forests: the EUROFLUX methodology. Adv. Ecol. Res. 30, 113–175. https://doi.org/10.1016/S0065-2504(08)60018-5.

Austin, R.B., Kingston, G., Longden, P.C., Donovan, P.A., 1978. Gross energy yields and the support energy requirements for the production of sugar from beet and cane; a study of four production areas. J. Agric. Sci. 91, 667–675. https://doi.org/10.1017/S0021859600060068.

Bala, G., Caldeira, K., Mirin, A., Wickett, M., Delire, C., Phillips, T.J., 2006. Biogeophysical effects of CO_2 fertilization on global climate. Tellus, Series B: Chem. Phys. Meteorol. 620–627. https://doi.org/10.1111/j.1600-0889.2006.00210.x.

Baldocchi, D.D., 2020. How eddy covariance flux measurements have contributed to our understanding of Global Change Biology. Glob. Chang. Biol. 26, 242–260. https://doi.org/10.1111/gcb.14807.

Baldocchi, D.D., 2003. Assessing the eddy covariance technique for evaluating carbon dioxide exchange rates of ecosystems: past, present and future. Glob. Chang. Biol. 9, 479–492. https://doi.org/10.1046/j.1365-2486.2003.00629.x.

Baldocchi, D.D., Hicks, B.B., Meyers, T.P., 1988. Measuring biosphere-atmosphere exchanges of biologically related gases with micrometeorological methods. Ecology. 69. https://doi.org/10.2307/1941631.

Beer, C., Reichstein, M., Tomelleri, E., Ciais, P., Jung, M., Carvalhais, N., Rödenbeck, C., Arain, M.A., Baldocchi, D., Bonan, G.B., Bondeau, A., Cescatti, A., Lasslop, G., Lindroth, A., Lomas, M., Luyssaert, S., Margolis, H., Oleson, K.W., Roupsard, O., Veenendaal, E., Viovy, N., Williams, C., Woodward, F.I., Papale, D., 2010. Terrestrial gross carbon dioxide uptake: global distribution and covariation with climate. Science (1979) 329. https://doi.org/10.1126/science.1184984, 1979.

Carvalhais, N., Forkel, M., Khomik, M., Bellarby, J., Jung, M., Migliavacca, M., Mu, M., Saatchi, S., Santoro, M., Thurner, M., Weber, U., Ahrens, B., Beer, C., Cescatti, A., Randerson, J.T., Reichstein, M., 2014. Global covariation of carbon turnover times with climate in terrestrial ecosystems. Nature 514, 213–217. https://doi.org/10.1038/nature13731.

Chang, C.W., Ushio, M., Hsieh, C.hao, 2017. Empirical dynamic modeling for beginners. Ecol. Res. 32. https://doi.org/10.1007/s11284-017-1469-9.

Chayawat, C., Satakhun, D., Kasemsap, P., Sathornkich, J., Phattaralerphong, J., 2019. Environmental controls on net CO_2 exchange over a young rubber plantation in northeastern Thailand. ScienceAsia 45. https://doi.org/10.2306/scienceasia1513-1874.2019.45.050.

Chen, Y., Guan, Y., Shao, G., Zhang, D., 2016. Investigating trends in streamflow and precipitation in Huangfuchuan basin with wavelet analysis and the Mann-Kendall test. Water (Switzerland) 8. https://doi.org/10.3390/w8030077.

Chen, Z., Yu, G., Wang, Q., 2019. Magnitude, pattern and controls of carbon flux and carbon use efficiency in China's typical forests. Glob. Planet. Change 172, 464–473. https://doi.org/10.1016/j.gloplacha.2018.11.004.

Cheng, J., Xie, M., 2008. The analysis of regional climate change features over Yunnan in recent 50 years. Prog. Geogr. 5, 19.

Ciais, P., Piao, S.L., Cadule, P., Friedlingstein, P., Chédin, A., 2009. Variability and recent trends in the African terrestrial carbon balance. Biogeosciences. 6. https://doi.org/10.5194/bg-6-1935-2009.

Clough, Y., Krishna, V.V., Corre, M.D., Darras, K., Denmead, L.H., Meijide, A., Moser, S., Musshoff, O., Steinebach, S., Veldkamp, E., Allen, K., Barnes, A.D., Breidenbach, N., Brose, U., Buchori, D., Daniel, R., Finkeldey, R., Harahap, I., Hertel, D., Holtkamp, A. M., Hörandl, E., Irawan, B., Jaya, I.N.S., Jochum, M., Klarner, B., Knohl, A., Kotowska, M.M., Krashevska, V., Kreft, H., Kurniawan, S., Leuschner, C., Maraun, M., Melati, D.N., Opfermann, N., Pérez-Cruzado, C., Prabowo, W.E., Rembold, K., Rizali, A., Rubiana, R., Schneider, D., Tjitrosoedirdjo, S.S., Tjoa, A., Tscharntke, T., Scheu, S., 2016. Land-use choices follow profitability at the expense of ecological functions in Indonesian smallholder landscapes. Nat. Commun. 7. https://doi.org/10.1038/ncomms13137.

Falge, E., Baldocchi, D., Olson, R., Anthoni, P., Aubinet, M., Bernhofer, C., Burba, G., Ceulemans, R., Clement, R., Dolman, H., Granier, A., Gross, P., Grünwald, T., Hollinger, D., Jensen, N.O., Katul, G., Keronen, P., Kowalski, A., Lai, C.T., Law, B.E., Meyers, T., Moncrieff, J., Moors, E., Munger, J.W., Pilegaard, K., Rannik, Ü., Rebmann, C., Suyker, A., Tenhunen, J., Tu, K., Verma, S., Vesala, T., Wilson, K., Wofsy, S., 2001. Gap filling strategies for defensible annual sums of net ecosystem exchange. Agric. For. Meteorol. 107. https://doi.org/10.1016/S0168-1923(00)00225-2.

Fang, C., Moncrieff, J.B., 2001. The dependence of soil CO_2 efflux on temperature. Soil. Biol. Biochem. 33. https://doi.org/10.1016/S0038-0717(00)00125-5.

Fei, X., Song, Q., Zhang, Y., Liu, Y., Sha, L., Yu, G., Zhang, L., Duan, C., Deng, Y., Wu, C., Lu, Z., Luo, K., Chen, A., Xu, K., Liu, W., Huang, H., Jin, Y., Zhou, R., Li, J., Lin, Y., Zhou, L., Fu, Y., Bai, X., Tang, X., Gao, J., Zhou, W., Grace, J., 2018. Carbon exchanges and their responses to temperature and precipitation in forest ecosystems in Yunnan, Southwest China. Sci. Total. Environ. 616–617. https://doi.org/10.1016/j.scitotenv.2017.10.239.

Fei, X., Song, Q., Zhang, Y., Yu, G., Zhang, L., Sha, L., Liu, Y., Xu, K., Chen, H., Wu, C., Chen, A., Zhang, S., Liu, W., Huang, H., Deng, Y., Qin, H., Li, P., Grace, J., 2019. Patterns and controls of light use efficiency in four contrasting forest ecosystems in Yunnan, southwest China. J. Geophys. Res. Biogeosci. 124. https://doi.org/10.1029/2018JG004487.

Feldpausch, T.R., Phillips, O.L., Brienen, R.J.W., Gloor, E., Lloyd, J., Lopez-Gonzalez, G., Monteagudo-Mendoza, A., Malhi, Y., Alarcón, A., Álvarez Dávila, E., Alvarez-Loayza, P., Andrade, A., Aragao, L.E.O.C., Arroyo, L., Aymard, C., G.A., Baker, T.R., Baraloto, C., Barroso, J., Bonal, D., Castro, W., Chama, V., Chave, J., Domingues, T. F., Fauset, S., Groot, N., Honorio Coronado, E., Laurance, S., Laurance, W.F., Lewis, S.L., Licona, J.C., Marimon, B.S., Marimon-Junior, B.H., Mendoza Bautista, C., Neill, D.A., Oliveira, E.A., Oliveira dos Santos, C., Pallqui Camacho, N.C., Pardo-Molina, G., Prieto, A., Quesada, C.A., Ramírez, F., Ramírez-Angulo, H., Réjou-Méchain, M., Rudas, A., Saiz, G., Salomão, R.P., Silva-Espejo, J.E., Silveira, M., ter Steege, H., Stropp, J., Terborgh, J., Thomas-Caesar, R., van der Heijden, G.M.F., Vásquez Martinez, R., Vilanova, E., Vos, V.A., 2016. Amazon forest response to repeated droughts. Global. Biogeochem. Cycles. 30. https://doi.org/10.1002/2015GB005133.

Feng, Y., Zeng, Z., Searchinger, T.D., Ziegler, A.D., Wu, J., Wang, D., He, X., Elsen, P.R., Ciais, P., Xu, R., Guo, Z., Peng, L., Tao, Y., Spracklen, D.V., Holden, J., Liu, X., Zheng, Y., Xu, P., Chen, J., Jiang, X., Song, X.P., Lakshmi, V., Wood, E.F., Zheng, C., 2022. Doubling of annual forest carbon loss over the tropics during the early twenty-first century. Nat. Sustain. 5, 444–451. https://doi.org/10.1038/s41893-022-00854-3.

Fernández-Martínez, M., Sardans, J., Chevallier, F., Ciais, P., Obersteiner, M., Vicca, S., Canadell, J.G., Bastos, A., Friedlingstein, P., Sitch, S., Piao, S.L., Janssens, I.A., Peñuelas, J., 2019. Global trends in carbon sinks and their relationships with CO_2 and temperature. Nat. Clim. Chang. 9, 73–79. https://doi.org/10.1038/s41558-018-0367-7.

Gilmanov, T.G., Soussana, J.F., Aires, L., Allard, V., Ammann, C., Balzarolo, M., Barcza, Z., Bernhofer, C., Campbell, C.L., Cernusca, A., Cescatti, A., Clifton-Brown, J., Dirks, B.O.M., Dore, S., Eugster, W., Fuhrer, J., Gimeno, C., Gruenwald, T., Haszpra, L., Hensen, A., Ibrom, A., Jacobs, A.F.G., Jones, M.B., Lanigan, G., Laurila, T., Lohila, A., Manca, G., Marcolla, B., Nagy, Z., Pilegaard, K., Pinter, K., Pio, C., Raschi, A., Rogiers, N., Sanz, M.J., Stefani, P., Sutton, M., Tuba, Z., Valentini, R., Williams, M.L., Wohlfahrt, G., 2007. Partitioning European grassland net ecosystem CO_2 exchange into gross primary productivity and ecosystem respiration using light response function analysis. Agric. Ecosyst. Environ. 121. https://doi.org/10.1016/j.agee.2006.12.008.

Goldberg, S.D., Zhao, Y., Harrison, R.D., et al., 2017. Soil respiration in sloping rubber plantations and tropical natural forests in Xishuangbanna, China. Agr Ecosyst. Environ. 249, 237–246. https://doi.org/10.1016/j.agee.2017.08.001.

Hikosaka, K., Ishikawa, K., Borjigidai, A., Muller, O., Onoda, Y., 2006. Temperature acclimation of photosynthesis: mechanisms involved in the changes in temperature dependence of photosynthetic rate. J. Exp. Bot. 5, 291–302. https://doi.org/10.1093/jxb/erj049.

Hubau, W., Lewis, S.L., Phillips, O.L., Affum-Baffoe, K., Beeckman, H., Cuní-Sanchez, A., Daniels, A.K., Ewango, C.E.N., Fauset, S., Mukinzi, J.M., Sheil, D., Sonké, B., Sullivan, M.J.P., Sunderland, T.C.H., Taedoumg, H., Thomas, S.C., White, L.J.T., Abernethy, K.A., Adu-Bredu, S., Amani, C.A., Baker, T.R., Banin, L.F., Baya, F., Begne, S.K., Bennett, A.C., Benedet, F., Bitariho, R., Bocko, Y.E., Boeckx, P., Boundja, P., Brienen, R.J.W., Brncic, T., Chezeaux, E., Chuyong, G.B., Clark, C.J., Collins, M., Comiskey, J.A., Coomes, D.A., Dargie, G.C., de Haulleville, T., Kamdem, M.N.D., Doucet, J.L., Esquivel-Muelbert, A., Feldpausch, T.R., Fofanah, A., Foli, E.G., Gilpin, M., Gloor, E., Gonmadje, C., Gourlet-Fleury, S., Hall, J.S., Hamilton, A.C., Harris, D.J., Hart, T.B., Hockemba, M.B.N., Hladik, A., Ifo, S.A., Jeffery, K.J., Jucker, T., Yakusu, E.K., Kearsley, E., Kenfack, D., Koch, A., Leal, M.E., Levesley, A., Lindsell, J.A., Lisingo, J., Lopez-Gonzalez, G., Lovett, J.C., Makana, J. R., Malhi, Y., Marshall, A.R., Martin, J., Martin, E.H., Mbayu, F.M., Medjibe, V.P., Mihindou, V., Mitchard, E.T.A., Moore, S., Munishi, P.K.T., Bengone, N.N., Ojo, L., Ondo, F.E., Peh, K.S.H., Pickavance, G.C., Poulsen, A.D., Poulsen, J.R., Qie, L., Reitsma, J., Rovero, F., Swaine, M.D., Talbot, J., Taplin, J., Taylor, D.M., Thomas, D. W., Toirambe, B., Mukendi, J.T., Tuagben, D., Umunay, P.M., van der Heijden, G.M. F., Verbeeck, H., Vleminckx, J., Willcock, S., Wöll, H., Woods, J.T., Zemagho, L., 2020. Asynchronous carbon sink saturation in African and Amazonian tropical forests. Nature 579, 80–87. https://doi.org/10.1038/s41586-020-2035-0.

IPBES-IPCC, 2020. Biodiversity and Climate change: scientific outcome. Ipbes-Ipcc Co-Sponsored Workshop.

IPCC, 2023. Intergovernmental Panel on Climate Change - AR6 synthesis report: climate Change 2023, Climate Change 2022 – Impacts. Adapt. Vulnerabil.

Jarvis, P., Rey, A., Petsikos, C., Wingate, L., Rayment, M., Pereira, J., Banza, J., David, J., Miglietta, F., Borghetti, M., Manca, G., Valentini, R., 2007. Drying and wetting of Mediterranean soils stimulates decomposition and carbon dioxide emission: the "Birch effect. Tree Physiol. 27, 929–940. https://doi.org/10.1093/treephys/27.7.929.

Jin, Y., Liu, Y., Liu, J., Zhang, X., 2022. Energy balance closure problem over a tropical seasonal rainforest in Xishuangbanna, Southwest China: role of latent heat flux. Water (Switzerland) 14. https://doi.org/10.3390/w14030395.

Kaewthongrach, R., Chidthaisong, A., Charuchittipan, D., Vitasse, Y., Sanwangsri, M., Varnakovida, P., Diloksumpun, S., Panuthai, S., Pakoktom, T., Suepa, T., LeClerc, M. Y., 2020. Impacts of a strong El Niño event on leaf phenology and carbon dioxide exchange in a secondary dry dipterocarp forest. Agric. For. Meteorol. 287. https://doi.org/10.1016/j.agrformet.2020.107945.

Knauer, J., Zaehle, S., Reichstein, M., Medlyn, B.E., Forkel, M., Hagemann, S., Werner, C., 2017. The response of ecosystem water-use efficiency to rising atmospheric CO_2 concentrations: sensitivity and large-scale biogeochemical implications. New Phytol. 213. https://doi.org/10.1111/nph.14288.

Kosugi, Y., Takanashi, S., Ohkubo, S., Matsuo, N., Tani, M., Mitani, T., Tsutsumi, D., Nik, A.R., 2008. CO_2 exchange of a tropical rainforest at Pasoh in Peninsular Malaysia. Agric. For. Meteorol. 148. https://doi.org/10.1016/j.agrformet.2007.10.007.

Kosugi, Y., Takanashi, S., Tani, M., Ohkubo, S., Matsuo, N., Itoh, M., Noguchi, S., Nik, A. R., 2012. Effect of inter-annual climate variability on evapotranspiration and canopy CO_2 exchange of a tropical rainforest in Peninsular Malaysia. J. For. Res. 17, 227–240. https://doi.org/10.1007/s10310-010-0235-4.

Kupers, S.J., Wirth, C., Engelbrecht, B.M.J., Rüger, N., 2019. Dry season soil water potential maps of a 50 hectare tropical forest plot on Barro Colorado Island. Panama. Sci. Data 6. https://doi.org/10.1038/s41597-019-0072-z.

Kwon, H., Pendall, E., Ewers, B.E., Cleary, M., Naithani, K., 2008. Spring drought regulates summer net ecosystem CO_2 exchange in a sagebrush-steppe ecosystem. Agric. For. Meteorol. 148, 381–391. https://doi.org/10.1016/j.agrformet.2007.09.010.

Law, B.E., Thornton, P.E., Irvine, J., Anthoni, P.M., Van Tuyl, S., 2001. Carbon storage and fluxes in ponderosa pine forests at different developmental stages. Glob. Chang. Biol. 7, 755–777. https://doi.org/10.1046/j.1354-1013.2001.00439.x.

Lawrence, D., Coe, M., Walker, W., Verchot, L., Vandecar, K., 2022. The unseen effects of deforestation: biophysical effects on climate. Front for Glob change 5. https://doi.org/10.3389/ffgc.2022.756115.

Leakey, A.D.B., Ainsworth, E.A., Bernacchi, C.J., Rogers, A., Long, S.P., Ort, D.R., 2009. Elevated CO_2 effects on plant carbon, nitrogen, and water relations: six important lessons from FACE. J. Exp. Bot. 20, 2859–2876. https://doi.org/10.1093/jxb/erp096.

Lee, J.E., Frankenberg, C., Van Der Tol, C., Berry, J.A., Guanter, L., Boyce, C.K., Fisher, J. B., Morrow, E., Worden, J.R., Asefi, S., Badgley, G., Saatchi, S., 2013. Forest productivity and water stress in Amazonia: observations from GOSAT chlorophyll fluorescence. Tohoku J. Exp. Med. 230. https://doi.org/10.1098/rspb.2013.0171.

Lewis, S.L., Lopez-Gonzalez, G., Sonké, B., Affum-Baffoe, K., Baker, T.R., Ojo, L.O., Phillips, O.L., Reitsma, J.M., White, L., Comiskey, J.A., Djuikouo, K, M.N., Ewango, C.E.N., Feldpausch, T.R., Hamilton, A.C., Gloor, M., Hart, T., Hladik, A., Lloyd, J., Lovett, J.C., Makana, J.R., Malhi, Y., Mbago, F.M., Ndangalasi, H.J., Peacock, J., Peh, K.S.H., Sheil, D., Sunderland, T., Swaine, M.D., Taplin, J., Taylor, D., Thomas, S.C., Votere, R., Wöll, H., 2009. Increasing carbon storage in intact African tropical forests. Nature 457. https://doi.org/10.1038/nature07771.

Lewis, Simon L., Malhi, Y., Phillips, O.L., 2004a. Fingerprinting the impacts of global change on tropical forests. Philos. Trans. R. Soc. B: Biol. Sci. 359, 437–462. https://doi.org/10.1098/rstb.2003.1432.

Lewis, S.L., Phillips, O.L., Baker, T.R., Lloyd, J., Malhi, Y., Almeida, S., Higuchi, N., Laurance, W.F., Neill, D.A., Silva, J.N.M., Terborgh, J., Lezama, A.T., Martínez, R.V., Brown, S., Chave, J., Kuebler, C., Vargas, P.N., Vinceti, B., 2004b. Concerted changes in tropical forest structure and dynamics: evidence from 50 South American long-term plots. Philos. Trans. R. Soc. B: Biol. Sci. 359, 421–436. https://doi.org/10.1098/rstb.2003.1431.

Li, H., Ma, Y., Aide, T.M., Liu, W., 2008. Past, present and future land-use in Xishuangbanna, China and the implications for carbon dynamics. For. Ecol. Manage 255, 16–24. https://doi.org/10.1016/j.foreco.2007.06.051.

Li, X., Zhou, Z., Ma, S., Xu, H., Li, Y., Chen, D., 2018. Long-term decline of carbon sink and its underlying mechanisms in tropical montane rainforest of Jianfengling, Hainnan Island. Bull. Bot. Res. 38, 766–774.
Li, Z., Zhang, Y., Wang, S., Yuan, G., Yang, Y., Cao, M., 2010. Evapotranspiration of a tropical rain forest in Xishuangbanna, southwest China. Hydrol. Process. 24. https://doi.org/10.1002/hyp.7643.
Liu, W., Meng, F.R., Zhang, Y., Liu, Y., Li, H., 2004. Water input from fog drip in the tropical seasonal rain forest of Xishuangbanna, South-West China. J. Trop. Ecol. 20. https://doi.org/10.1017/S0266467404001890.
Liu, W., Zhang, Y., Liu, Y., Li, H., Duan, W., 2003. Comparison of fog interception at a tropical seasonal rain forest and a rubber plantation in Xishuangbanna, Southwest China. Acta Ecol. Sinica 11, 2379–2386.
Lloyd, J., Taylor, J.A., 1994. On the temperature dependence of soil respiration. Funct. Ecol. 8, 315–323. https://doi.org/10.2307/2389824.
Lyu, M., Giardina, C.P., Litton, C.M., 2021. Interannual variation in rainfall modulates temperature sensitivity of carbon allocation and flux in a tropical montane wet forest. Glob. Chang. Biol. 27, 3824–3836. https://doi.org/10.1111/gcb.15664.
Ma, Y., Wang, W., Jin, S., Li, Haoxin, Liu, B., Gong, W., Fan, R., Li, Hui, 2023. Spatiotemporal variation of LAI in different vegetation types and its response to climate change in China from 2001 to 2020. Ecol. Indic. 156. https://doi.org/10.1016/j.ecolind.2023.111101.
Mackey, B., Kormos, C.F., Keith, H., Moomaw, W.R., Houghton, R.A., Mittermeier, R.A., Hole, D., Hugh, S., 2020. Understanding the importance of primary tropical forest protection as a mitigation strategy. Mitig. Adapt. Strateg. Glob. Chang. 25, 763–787. https://doi.org/10.1007/s11027-019-09891-4.
Maia, V.A., Miranda Santos, A.B., de Aguiar-Campos, N., de Souza, C.R., de Oliveira, M. C.F., Coelho, P.A., Morel, J.D., da Costa, L.S., Farrapo, C.L., Alencar Fagundes, N.C., Pires de Paula, G.G., Santos, P.F., Gianasi, F.M., da Silva, W.B., de Oliveira, F., Girardelli, D.T., Araújo, F., de, C., Vilela, T.A., Pereira, R.T., Arantes da Silva, L.C., de Oliveira Menino, G.C., Garcia, P.O., Leite Fontes, M.A., dos Santos, R.M., 2020. The carbon sink of tropical seasonal forests in southeastern Brazil can be under threat. Sci. Adv. 6. https://doi.org/10.1126/SCIADV.ABD4548.
Malhi, Y., 2012. The productivity, metabolism and carbon cycle of tropical forest vegetation. J. Ecol. https://doi.org/10.1111/j.1365-2745.2011.01916.x.
Martínez-Vilalta, J., Poyatos, R., Aguadé, D., Retana, J., Mencuccini, M., 2014. A new look at water transport regulation in plants. New. Phytol. 204, 105–115. https://doi.org/10.1111/nph.12912.
Marvin, D.C., Sleeter, B.M., Cameron, D.R., Nelson, E., Plantinga, A.J., 2023. Natural climate solutions provide robust carbon mitigation capacity under future climate change scenarios. Sci. Rep. 13. https://doi.org/10.1038/s41598-023-43118-6.
Mi, N., Yu, G., Wang, P., Wen, X., Sun, X., 2006. A preliminary study for spatial representiveness of flux observation at ChinaFLUX sites. Sci. China Ser. D. Earth. Sci. 49. https://doi.org/10.1007/s11430-006-8024-9.
Mitchard, E.T.A., 2018. The tropical forest carbon cycle and climate change. Nature 559, 527–534. https://doi.org/10.1038/s41586-018-0300-2.
Monteith, J., Unsworth, M., 2013. Principles of environmental Physics: plants, animals, and the atmosphere: fourth edition, Principles of environmental Physics: plants, animals, and the atmosphere: fourth edition. https://doi.org/10.1016/C2010-0-66393-0.
Mori, A.S., Dee, L.E., Gonzalez, A., Ohashi, H., Cowles, J., Wright, A.J., Loreau, M., Hautier, Y., Newbold, T., Reich, P.B., Matsui, T., Takeuchi, W., Okada, K.ichi, Seidl, R., Isbell, F., 2021. Biodiversity–productivity relationships are key to nature-based climate solutions. Nat. Clim. Chang. 11, 543–550. https://doi.org/10.1038/s41558-021-01062-1.
Morton, D.C., Nagol, J., Carabajal, C.C., Rosette, J., Palace, M., Cook, B.D., Vermote, E.F., Harding, D.J., North, P.R.J., 2014. Amazon forests maintain consistent canopy structure and greenness during the dry season. Nature 506, 221–224. https://doi.org/10.1038/nature13006.
O'Connell, C.S., Ruan, L., Silver, W.L., 2018. Drought drives rapid shifts in tropical rainforest soil biogeochemistry and greenhouse gas emissions. Nat. Commun. 9. https://doi.org/10.1038/s41467-018-03352-3.
Pan, Y., Birdsey, R.A., Fang, J., Houghton, R., Kauppi, P.E., Kurz, W.A., Phillips, O.L., Shvidenko, A., Lewis, S.L., Canadell, J.G., Ciais, P., Jackson, R.B., Pacala, S.W., McGuire, A.D., Piao, S., Rautiainen, A., Sitch, S., Hayes, D., 2011. A large and persistent carbon sink in the world's forests. Science (1979) 333. https://doi.org/10.1126/science.1201609, 1979.
Pan, Y., Birdsey, R.A., Phillips, O.L., Houghton, R.A., Fang, J., Kauppi, P.E., Keith, H., Kurz, W.A., Ito, A., Lewis, S.L., Nabuurs, G.J., Shvidenko, A., Hashimoto, S., Lerink, B., Schepaschenko, D., Castanho, A., Murdiyarso, D., 2024. The enduring world forest carbon sink. Nature 631, 563–569. https://doi.org/10.1038/s41586-024-07602-x.
Pangle, L., Vose, J.M., Teskey, R.O., 2009. Radiation use efficiency in adjacent hardwood and pine forests in the southern Appalachians. For. Ecol. Manage 257, 1034–1042. https://doi.org/10.1016/j.foreco.2008.11.004.
Parsons, S.A., Valdez-Ramirez, V., Congdon, R.A., Williams, S.E., 2014. Contrasting patterns of litterfall seasonality and seasonal changes in litter decomposability in a tropical rainforest region. Biogeosciences. 11, 5047–5056. https://doi.org/10.5194/bg-11-5047-2014.
Peng, J., Tang, J., Xie, S., Wang, Y., Liao, J., Chen, C., Sun, C., Mao, J., Zhou, Q., Niu, S., 2024. Evidence for the acclimation of ecosystem photosynthesis to soil moisture. Nat. Commun. 15, 9795. https://doi.org/10.1038/s41467-024-54156-7.
Qi, Y., Fang, S., Zhou, W., 2014. Variation and spatial distribution of surface solar radiation in China over recent 50 years. Acta Ecol. Sinica 34. https://doi.org/10.5846/stxb201303130409.
Raich, J.W., Russell, A.E., Kitayama, K., Parton, W.J., Vitousek, P.M., 2006. Temperature influences carbon accumulation in moist tropical forests. Ecology. 87, 76–87. https://doi.org/10.1890/05-0023.
Rap, A., Spracklen, D.V., Mercado, L., Reddington, C.L., Haywood, J.M., Ellis, R.J., Phillips, O.L., Artaxo, P., Bonal, D., Restrepo Coupe, N., Butt, N., 2015. Fires increase Amazon forest productivity through increases in diffuse radiation. Geophys. Res. Lett. 42. https://doi.org/10.1002/2015GL063719.
Reichstein, M., Falge, E., Baldocchi, D., Papale, D., Aubinet, M., Berbigier, P., Bernhofer, C., Buchmann, N., Gilmanov, T., Granier, A., Grünwald, T., Havránková, K., Ilvesniemi, H., Janous, D., Knohl, A., Laurila, T., Lohila, A., Loustau, D., Matteucci, G., Meyers, T., Miglietta, F., Ourcival, J.M., Pumpanen, J., Rambal, S., Rotenberg, E., Sanz, M., Tenhunen, J., Seufert, G., Vaccari, F., Vesala, T., Yakir, D., Valentini, R., 2005. On the separation of net ecosystem exchange into assimilation and ecosystem respiration: review and improved algorithm. Glob. Chang. Biol. 11, 1424–1439. https://doi.org/10.1111/j.1365-2486.2005.001002.x.
Restrepo-Coupe, N., da Rocha, H.R., Hutyra, L.R., da Araujo, A.C., Borma, L.S., Christoffersen, B., Cabral, O.M.R., de Camargo, P.B., Cardoso, F.L., da Costa, A.C.L., Fitzjarrald, D.R., Goulden, M.L., Kruijt, B., Maia, J.M.F., Malhi, Y.S., Manzi, A.O., Miller, S.D., Nobre, A.D., von Randow, C., Sá, L.D.A., Sakai, R.K., Tota, J., Wofsy, S. C., Zanchi, F.B., Saleska, S.R., 2013. What drives the seasonality of photosynthesis across the Amazon basin? A cross-site analysis of eddy flux tower measurements from the Brasil flux network. Agric. For. Meteorol. 182, 128–144. https://doi.org/10.1016/j.agrformet.2013.04.031.
Rodda, S.R., Thumaty, K.C., Praveen, M.S.S., Jha, C.S., Dadhwal, V.K., 2021. Multi-year eddy covariance measurements of net ecosystem exchange in tropical dry deciduous forest of India. Agric. For. Meteorol. 301–302. https://doi.org/10.1016/j.agrformet.2021.108351.
Rodrigues, S., Cirino, G., Moreira, D., Pozzer, A., Palácios, R., Lee, S.C., Imbiriba, B., Nogueira, J., Vitorino, M.I., Vourlitis, G., 2024. Enhanced net CO2 exchange of a semideciduous forest in the southern Amazon due to diffuse radiation from biomass burning. Biogeosciences. 21. https://doi.org/10.5194/bg-21-843-2024.
Ruehr, S., Keenan, T.F., Williams, C., Zhou, Y., Lu, X., Bastos, A., Canadell, J.G., Prentice, I.C., Sitch, S., Terrer, C., 2023. Evidence and attribution of the enhanced land carbon sink. Nat. Rev. Earth. Environ. 4, 518–534. https://doi.org/10.1038/s43017-023-00456-3.
Saigusa, N., Yamamoto, S., Hirata, R., Ohtani, Y., Ide, R., Asanuma, J., Gamo, M., Hirano, T., Kondo, H., Kosugi, Y., Li, S.G., Nakai, Y., Takagi, K., Tani, M., Wang, H., 2008. Temporal and spatial variations in the seasonal patterns of CO_2 flux in boreal, temperate, and tropical forests in East Asia. Agric. For. Meteorol. 148, 700–713. https://doi.org/10.1016/j.agrformet.2007.12.006.
Saleska, S.R., Miller, S.D., Matross, D.M., Goulden, M.L., Wofsy, S.C., Da Rocha, H.R., De Camargo, P.B., Crill, P., Daube, B.C., De Freitas, H.C., Hutyra, L., Keller, M., Kirchhoff, V., Menton, M., Munger, J.W., Pyle, E.H., Rice, A.H., Silva, H., 2003. Carbon in Amazon forests: unexpected seasonal fluxes and disturbance-induced losses. Science (1979) 302. https://doi.org/10.1126/science.1091165.
Sanwangsri, M., Suwannapat, P., Chidthaisong, A., Komori, D., Suwanapat, P., Kim, W., 2018. Net ecosystem CO2 exchange over a dry dipterocarp forest in Phayao, northern Thailand.
Sayer, E.J., Powers, J.S., Tanner, E.V.J., 2007. Increased litterfall in tropical forests boosts the transfer of soil CO_2 to the atmosphere. PLoS. One 2. https://doi.org/10.1371/journal.pone.0001299.
Scheffer, M., Bascompte, J., Brock, W.A., Brovkin, V., Carpenter, S.R., Dakos, V., Held, H., Van Nes, E.H., Rietkerk, M., Sugihara, G., 2009. Early-warning signals for critical transitions. Nature 461, 53–59. https://doi.org/10.1038/nature08227.
Schuur, E.A.G., 2003. Productivity and global climate revisited: the sensitivity of tropical forest growth to precipitation. Ecology. 84, 1165–1170. https://doi.org/10.1890/0012-9658(2003)084[1165:PAGCRT]2.0.CO;2.
Seddon, A.W.R., Macias-Fauria, M., Long, P.R., Benz, D., Willis, K.J., 2016. Sensitivity of global terrestrial ecosystems to climate variability. Nature 531, 229–232. https://doi.org/10.1038/nature16986.
Shi, H., Li, L., Eamus, D., Cleverly, J., Huete, A., Beringer, J., Yu, Q., Van Gorsel, E., Hutley, L., 2014. Intrinsic climate dependency of ecosystem light and water-use-efficiencies across Australian biomes. Environ. Res. Lett. 9. https://doi.org/10.1088/1748-9326/9/10/104002.
Singh, A., Agrawal, M., 2015. Effects of ambient and elevated CO_2 on growth, chlorophyll fluorescence, photosynthetic pigments, antioxidants, and secondary metabolites of Catharanthus roseus (L.) G Don. Grown under three different soil N levels. Environ. Sci. Pollut. Res. 22, 3936–3946. https://doi.org/10.1007/s11356-014-3661-6.
Sohel, M.S.I., Grau, A.V., McDonnell, J.J., Herbohn, J., 2021. Tropical forest water source patterns revealed by stable isotopes: a preliminary analysis of 46 neighboring species. For. Ecol. Manage 494. https://doi.org/10.1016/j.foreco.2021.119355.
Sugihara, G., May, R., Ye, H., Hsieh, C.H., Deyle, E., Fogarty, M., Munch, S., 2012. Detecting causality in complex ecosystems. Science (1979) 338. https://doi.org/10.1126/science.1227079.
Takamura, N., Hata, Y., Matsumoto, K., Kume, T., Ueyama, M., Kumagai, T., 2023. El Niño-Southern Oscillation forcing on carbon and water cycling in a Bornean tropical rainforest. Proc. Natl. Acad. Sci. U S. A 120. https://doi.org/10.1073/pnas.2301596120.
Tan, Z., 2010. The Carbon Balance of a Primary Tropical Seasonal Rain Forest.
Tan, Z., Zhang, Y., Song, Q., Yu, G., Liang, N., 2014. Leaf shedding as an adaptive strategy for water deficit: a case study in Xishuangbannas rainforest. J. Yunnan Univ. Nat. Sci. 2, 273–280.
Tan, Z., Zhang, Y., Yu, G., Sha, L., Tang, J., Deng, X., Song, Q., 2010. Carbon balance of a primary tropical seasonal rain forest. J. Geophys. Res. Atmos. 115. https://doi.org/10.1029/2009JD012913.

Tanner, C.B., Thurtell, G.W., 1969. Anemoclinometer measurements of Reynolds stress and heat transport in the atmospheric surface layer.
Tharammal, T., Bala, G., Narayanappa, D., Nemani, R., 2019. Potential roles of CO_2 fertilization, nitrogen deposition, climate change, and land use and land cover change on the global terrestrial carbon uptake in the twenty-first century. Clim. Dyn. 52, 4393–4406. https://doi.org/10.1007/s00382-018-4388-8.
Tomimatsu, H., Iio, A., Adachi, M., Saw, L.G., Fletcher, C., Tang, Y., 2014. High CO_2 concentration increases relative leaf carbon gain under dynamic light in Dipterocarpus sublamellatus seedlings in a tropical rain forest. Malaysia. Tree Physiol. 34, 944–954. https://doi.org/10.1093/treephys/tpu066.
Ueyama, M., Iwata, H., Nagano, H., Kukuu, N., Harazono, Y., 2024. Anomalous wet summers and rising atmospheric CO_2 concentrations increase the CO_2 sink in a poorly drained forest on permafrost. Proc. Nat. Acad. Sci. U S A 121. https://doi.org/10.1073/pnas.2414539121.
Van der Molen, M.K., Dolman, A.J., Ciais, P., Eglin, T., Gobron, N., Law, B.E., Meir, P., Peters, W., Phillips, O.L., Reichstein, M., Chen, T., Dekker, S.C., Doubková, M., Friedl, M.A., Jung, M., van den Hurk, B.J.J.M., de Jeu, R.A.M., Kruijt, B., Ohta, T., Rebel, K.T., Plummer, S., Seneviratne, S.I., Sitch, S., Teuling, A.J., van der Werf, G. R., Wang, G., 2011. Drought and ecosystem carbon cycling. Agric. For. Meteorol. https://doi.org/10.1016/j.agrformet.2011.01.018.
Vourlitis, G.L., De Almeida Lobo, F., Zeilhofer, P., De Souza Nogueira, J., 2011. Temporal patterns of net CO_2 exchange for a tropical semideciduous forest of the southern Amazon Basin. J. Geophys. Res. Biogeosci. 116. https://doi.org/10.1029/2010JG001524.
Walker, A.P., De Kauwe, M.G., Bastos, A., et al., 2021. Integrating the evidence for a terrestrial carbon sink caused by increasing atmospheric CO_2. New. Phytol. https://doi.org/10.1111/nph.16866.
Wang, Y., Liu, J., Wennberg, P.O., He, L., Bonal, D., Köhler, P., Frankenberg, C., Sitch, S., Friedlingstein, P., 2023. Elucidating climatic drivers of photosynthesis by tropical forests. Glob. Chang. Biol. 29, 4811–4825. https://doi.org/10.1111/gcb.16837.
Wang, Q., Zhang, H., Yang, S., Chen, Q., Zhou, X., Shi, G., Cheng, Y., Wild, M., 2021. Potential driving factors on surface solar radiation trends over china in recent years. Remote Sens. (Basel) 13. https://doi.org/10.3390/rs13040704.
Waring, B.G., Powers, J.S., 2016. Unraveling the mechanisms underlying pulse dynamics of soil respiration in tropical dry forests. Environ. Res. Lett. 11. https://doi.org/10.1088/1748-9326/11/10/105005.
Wieder, W.R., Cleveland, C.C., Townsend, A.R., 2009. Controls over leaf litter decomposition in wet tropical forests. Ecology. 90, 3333–3341. https://doi.org/10.1890/08-2294.1.
Wolf, S., Eugster, W., Potvin, C., Buchmann, N., 2011. Strong seasonal variations in net ecosystem CO_2 exchange of a tropical pasture and afforestation in Panama. Agric. For. Meteorol. 151, 1139–1151. https://doi.org/10.1016/j.agrformet.2011.04.002.
Xiong, Q., Sun, Z., Cui, W., Lei, J., Fu, X., Wu, L., 2022. A study on sensitivities of tropical forest GPP responding to the characteristics of drought—A case study in Xishuangbanna, China. Water 14 (2), 157. https://doi.org/10.3390/w14020157.
Yan, J., Zhang, Y., Yu, G., Zhou, G., Zhang, L., Li, K., Tan, Z., Sha, L., 2013. Seasonal and inter-annual variations in net ecosystem exchange of two old-growth forests in southern China. Agric. For. Meteorol. 182, 257–265. https://doi.org/10.1016/j.agrformet.2013.03.002.
Yan, M., Li, Z.Y., Tian, X., Chen, E.X., Gu, C.Y., 2016. Remote sensing estimation of gross primary productivity and its response to climate change in the upstream of Heihe River Basin. Chin. J. Plant Ecol. 40, 1–12. https://doi.org/10.17521/cjpe.2015.0253.
Yao, P., Kou, W., Wang, Q., Han, Y., 2020. Relationship between climate change and rubber planting in Xishuangbanna in recent 60 years. For. Inventory Plann. 3, 17–23.
Yao, Y., Zhang, Y., Liang, N., Tan, Z., Yu, G., Sha, L., Song, Q., 2012. Pooling of CO2 within a small valley in a tropical seasonal rain forest. J. For. Res. 17, 241–252. https://doi.org/10.1007/s10310-011-0268-3.
Ye, H., Deyle, E.R., Gilarranz, L.J., Sugihara, G., 2015. Distinguishing time-delayed causal interactions using convergent cross mapping. Sci. Rep. 5. https://doi.org/10.1038/srep14750.
Yu, G., Wen, X., Sun, X., Tanner, B.D., Lee, X., Chen, J., 2006. Overview of ChinaFLUX and evaluation of its eddy covariance measurement. Agric. For. Meteorol. 137, 125–137. https://doi.org/10.1016/j.agrformet.2006.02.011.
Zeri, M., Sá, L.D.A., Manzi, A.O., Araú, A.C., Aguiar, R.G., Von Randow, C., Sampaio, G., Cardoso, F.L., Nobre, C.A., 2014. Variability of carbon and water fluxes following climate extremes over a tropical forest in southwestern amazonia. PLoS. One 9. https://doi.org/10.1371/journal.pone.0088130.
Zhang, J., Song, Q., Zhang, Y., Deng, Y., Wu, C., 2018. Characteristics of fog in Xishuangbanna tropical rainforest and Ailaoshan subtropical evergreen broad-leaved forest. Acta Ecol. Sinca 38, 8758–8765.
Zhang, L., Yu, G., Sun, X., Wen, X., Ren, C., Song, X., Liu, Y., Guan, D., Yan, J., Zhang, Y., 2006a. Seasonal variation of carbon exchange of typical forest ecosystems along the eastern forest transect in China. Sci. China Ser. D. Earth. Sci. 49. https://doi.org/10.1007/s11430-006-8047-2.
Zhang, M., 2009. Characteristic Parameters of Fluxes in a Tropical Seasonal Rainforest of Xishuangbanna, SW China.
Zhang, X., Zhang, Y., Sha, L., et al., 2015. Effects of continuous drought stress on soil respiration in a tropical rainforest in southwest China. Plant Soil. 394, 343–353. https://doi.org/10.1007/s11104-015-2523-4.
Zhang, X., Zhang, Y., Tian, J., Ma, N., Wang, Y.P., 2022. CO_2 fertilization is spatially distinct from stomatal conductance reduction in controlling ecosystem water-use efficiency increase. Environ. Res. Lett. 17. https://doi.org/10.1088/1748-9326/ac6c9c.
Zhang, Y., Holbrook, N.M., Cao, K., 2014. Seasonal dynamics in photosynthesis of woody plants at the northern limit of Asian tropics: potential role of fog in maintaining tropical rainforests and agriculture in Southwest China. Tree Physiol. 34, 1069–1078. https://doi.org/10.1093/treephys/tpu083.
Zhang, Y., Sha, L., Yu, G., Song, Q., Tang, J., Yang, X., Wang, Y., Zheng, Z., Zhao, S., Yang, Z., Sun, X., 2006b. Annual variation of carbon flux and impact factors in the tropical seasonal rain forest of Xishuangbanna, SW China. Sci. China Ser. D. Earth. Sci. 49, 150–162. https://doi.org/10.1007/s11430-006-8150-4.
Zhang, Y., Tan, Z., Song, Q., Yu, G., Sun, X., 2010. Respiration controls the unexpected seasonal pattern of carbon flux in an Asian tropical rain forest. Atmos. Environ. 44, 3886–3893. https://doi.org/10.1016/j.atmosenv.2010.07.027.
Zheng, Z., Li, Y., Liu, H., Feng, Z., Gan, J., Kong, W., 2005. Litterfall of tropical rain forests at different altitudes, Xishuangbanna, Southwest China. Acta Phytoecol. Sin. 6, 884–893.
Zhou, L., Song, Q., Zhang, Y., Fei, X., Deng, Y., Wu, C., Zhou, R., Lin, Y., Deng, X., Chen, A., Li, P., 2017. Comparison of net ecosystem exchange light-response curve fitted parameters at four types of forest ecosystems. Chin. J. Ecol. 36, 1815–1824.
Zhu, H., 1992. The tropical rainforest vegetation in Xishuangbanna. Chin. Geogr. Sci. 2. https://doi.org/10.1007/BF02664547.
Zhu, H., Wang, H., Li, B., Zhou, S., Zhang, J., 1998. Research on tropical seasonal rainforest of Xishuangbanna, south Yunnan. Guihaia 4, 372–384.